Chemical and mechanical analysis of Danubian *Myriophyllum spicatum*

Institute of Chemistry of Renewable Resources

University of Natural Resources and Life Sciences, Vienna

Vienna 2020

Supervisor: Rosenau, Thomas, Univ.Prof. Dipl.-Chem. Dr.rer.nat. Dr.h.c.
Co-supervisor: Beaumont, Marco, Dr.

Submitted for the degree Master of Science / Dipl.-Ing.

by

Patrick Geiger, BSc

Abstract

Myriophyllum spicatum is a highly invasive and fast-growing freshwater aquatic plant with a growing capacity of 20 tons per year and hectare in the region of Vienna, Austria. Currently, the plant is harvested with great effort to contain its growth. This huge amount of biomass is treated as biological waste and so far, it is just composted. The motivation of this thesis is to explore the energetic utilization of *M. spicatum* and its potential as source material for packaging materials.

In a first step, the macromolecular constituents of *M. spicatum* were determined. Its high holocellulose content of 44 %, consisting of cellulose as main component as well as hemicelluloses and pectin. Besides this fraction, the plant contained 11 % of lignin, which is rare in aquatic plants. Based on these findings, a pulping process was developed, to obtain a cellulose-rich pulp for material application. Paper produced from this pulp could withstand a tensile strength of up to 63 MPa without any additives. These results are comparable to the reference material, a softwood kraft pulp. Moreover, the addition of *M. spicatum*-based pulp to a softwood kraft pulp (in a 60:40 weight ratio) had an increased tensile strength of 70 MPa and increased the toughness, suggesting a synergetic effect of the two materials.

In parallel, the methane yield of this biomass in biogas production was investigated. 161 l of methane could be produced from one kg of dry biomass, which is an encouraging result and comparable to biomass production from plant waste.

All in all, the results in this thesis show that *M. spicatum* has a yet untapped potential for energetic and material utilization. It became clear that *M. spicatum* could replace wood or plastic as source material in packaging materials. Exploiting the potential of this inexpensive and ubiquitously available biomass for the proposed utilizations will be important in modern biorefinery approaches.

Acknowledgments

Index

List of figures

List of tables

List of abbreviations

AD	Anaerobic digestion
ATR-FTIR	Attenuated total reflectance Fourier-transformed infrared spectroscopy
BSTFA	N,O-Bis(trimethylsilyl)trifluoroacetamide
DMAP	4-Dimethylaminopyridine
DP	Degree of polymerization
EtOH	Ethanol
GalA	Galacturonic acid
GC-MS	Gas chromatography-mass spectroscopy
HG	Homogalacturonan
HPLC	High-performance liquid chromatography
HPTLC	High-performance thin layer chromatography
IEX	Ion exchange chromatography
LTBR	Liquid to biomass ratio
MeOH	Methanol
NMR	Nuclear magnetic resonance
ODM	Organic dry matter
PLA	Polylactic acid
RCF	Relative centrifugal force
RG	Rhamnogalacturonan
RPM	Revolutions per minute
RT	Room temperature
SD	Standard deviation
SEM	Scanning electron microscope
TAPPI	Technical Association of the Pulp and Paper Industry
TGA	Thermogravimetric analysis
TMCS	Trimethylsilyl chloride
Tol	Toluene

1.   Introduction

Nowadays, we are in the middle of a paradigm shift from an oil-based economy to an economy based on renewable resources and energies. i.e. bioeconomy. As a consequence, the research focus shifts more and more away from petroleum-based products towards sustainable and renewable alternatives. Suitable and environmentally benign materials can be produced by two different approaches:

(1) A bio-synthetic bottom-up approach, in which a biopolymer is synthesized form building blocks, e.g. the degradable bioplastic polylactic acid (PLA), which is synthesized from lactic acid and lactide via biofermentation (Södergård and Stolt 2010).

(2) Or a top-down approach, in which biopolymers like cellulose are extracted from a sustainable resource.

For both strategies it is important to find suitable starting materials to synthesize or extract the biopolymers from. In general, the bottom-up approach is looking for a cheap sugar source with good availability which is preferably not in direct competition with food production. While the top-down approach is seeking an inexpensive source of the respective biopolymer preferentially in high concentrations and from a non-wood material to ease the extraction process and discourage further deforestation.

In this work, *Myriophyllum spicatum* was studied as potential source material for cellulose-rich pulp: *M. spicatum* is a highly invasive, submerged aquatic plant which grows in still or slow-moving fresh water bodies in at least 57 countries worldwide (Murphy 2018). The city of Vienna, Austria has harvested 3,350 t of submerged plants in 2018 alone in order to allow for diverse river-side recreational activities. Figure 1 shows the harvest of M. spicatum using amphibious mowing boats at the Old Danube in Vienna.

This translates into a growing capacity of 20 tons per hectare and year. At the time of writing, all this potentially valuable material is merely disposed at a composting plant (Wiener Gewässer (Magistratsabteilung 45) 2019).

The chemical composition of *M. spicatum* was studied superficially in the literature (Marko et al. 2008) and recent studies focus rather on the plants biology than its possible utilization in materials science (Moody et al. 2016; He et al. 2016).

Therefore, the aim of this thesis is to investigate the chemical composition of *M. spicatum* and evaluate its potential for application in material sciences (as more sustainable alternative to conventional wood-derived pulp) and energetic utilization (biogas experiments).

Figure 1: Harvest of M. spicatum at the Old Danube, Vienna (Wiener Gewässer (Magistratsabteilung 45) 2019)

The following sections give a short introduction to the chemical composition of plant fiber and its comparison to wood fiber, to relevant parts of material testing and anaerobic digestion concerning the biogas experiments.

1.1 Chemical composition of plant fiber

Comparison between woody and aquatic *plant cells*

Figure 2 shows a schematic comparison between aquatic plant and woody cells. The most significant differences between woody and submarine plant cells lie in the size of their vacuoles and cell walls. While the vacuoles of woody plants encompass a relatively small area, the secondary cell wall is much more elaborated and expansive to be able to withstand the gravitational forces. Submarine plants have large vacuoles with high cellular pressure to stay afloat and a less developed secondary cell wall.
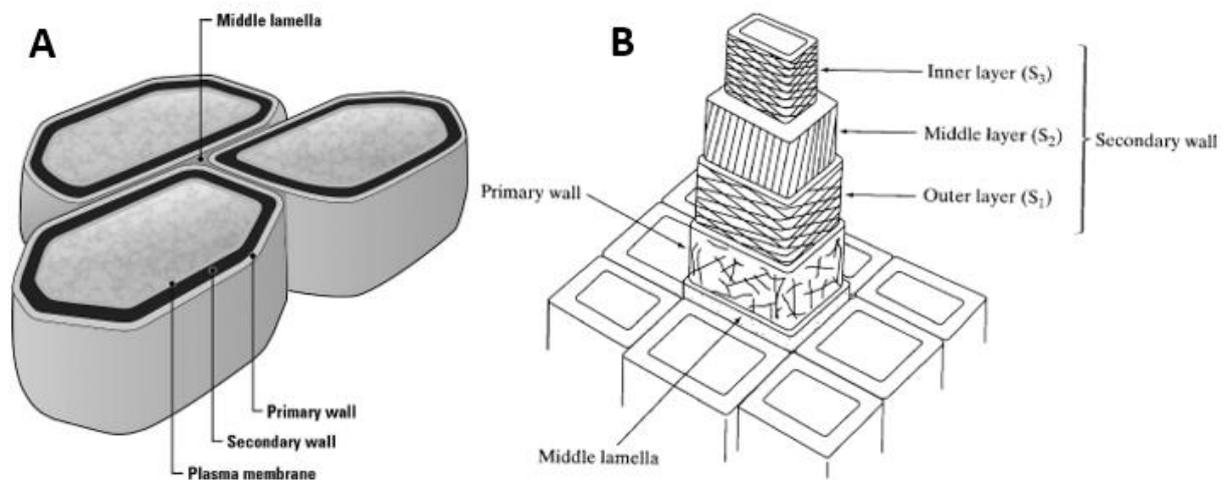
Figure 2: Schematic comparison between plant (A) and wood cells (B) (Dinwoodie 1989).

These two factors are well reflected in the moisture content of both plants: while wood usually contains 10-25 % of water, submarine plants contain up to 90 %.

Table 1 shows the chemical composition *M. spicatum* and softwood, which is the primary substrate for pulp and paper industry. On a dry weight basis, softwood contains significantly more holocellulose and lignin, while *M. spicatum* has additionally rather large amounts of protein and ash, which may influence the wet-chemistry analysis that is designed for wood samples. The amount of extractives is comparable between the two plants materials.

Table 1: Comparison of the chemical composition of softwood and M. spicatum (Marko et al. 2008, Serin et al. 2003).

Compontent	Softwood [%]	*M. spicatum* [%]
Holocellulose	60-70	53
Lignin	15-30	12
Extractives	2-10	11
Proteins	<1	17
Ash	0.5-1	8

Carbohydrates

The world's most abundant carbohydrate is the polysaccharide is cellulose. Cellulose consists of chains of anhydro-β-D-glucopyranose, which are covalently bound by β-1,4-glyosidic linkages and can reach degrees of polymerization of over 10,000 monosaccharide units. It forms semi-crystalline structures in fibrillar shape. The smallest subunit is defined as microfibril consisting of approximately 18-24 cellulose chains and has a diameter of approx. 3 nm. The microfibril is composed of crystalline and amorphous cellulose (see Figure 3). The cellulose crystal has an astonishing elastic modulus of 137-220 GPa, which is in the range of cast iron. In nature, cellulose is typically embedded in a fibrous blend structure with other heteromeric polysaccharides, mostly hemicellulose, pectin, and lignin. Hemicellulose and pectin are the cement and glue of the cell wall, tethering the individual cellulose fibrils (Ragnar et al. 2014; Shao and Wang 2018).
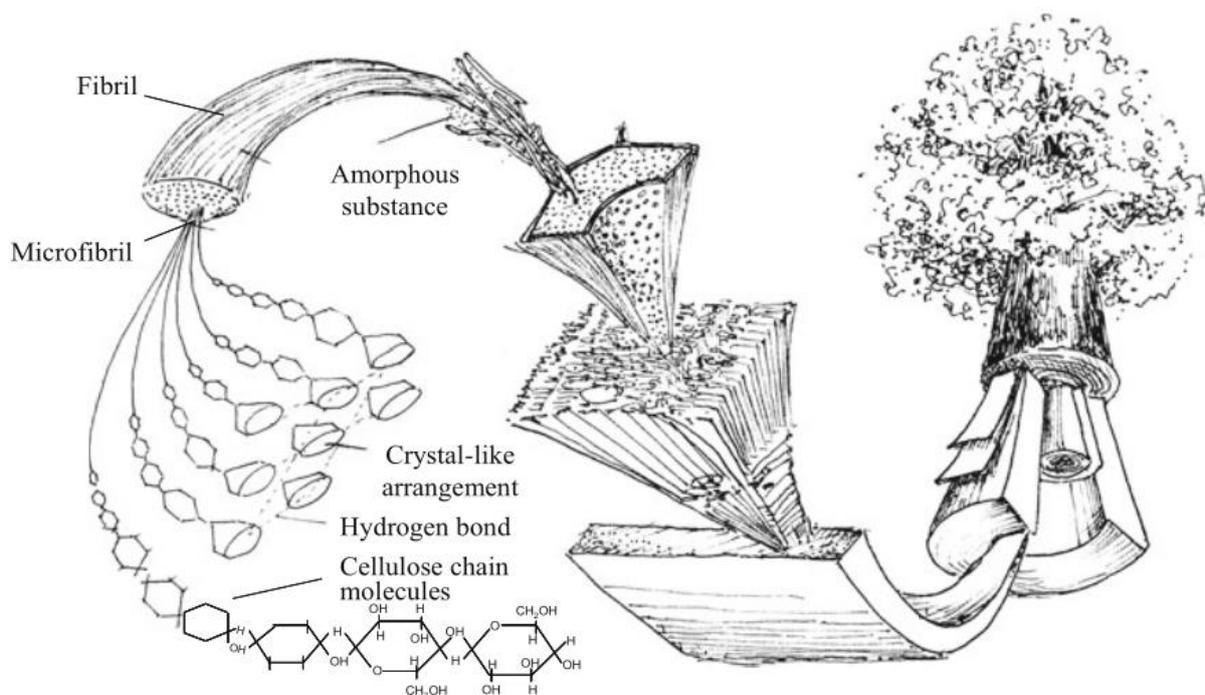
Figure 3: Schematic of a wood structure (Shao and Wang 2018).

Wood hemicelluloses display a lower molar mass than cellulose with a degree of polymerization (DP) in the range of 100 to 200. The two most important groups are xylans and glucomannans: xylans are generally considered as more chemically stable during the pulping process (compare Table 2) and are polysaccharides consisting of β-1,4-linked xylose units with side branches of α-arabinofuranose and α-glucuronic acids. The composition of glucomannans is different, they are composed of β-1,4-linked D-mannose and D-glucose as well as galactose in case of galactoglucomannans.

Another important plant component in the cell wall is pectins; a heterogeneous, branched and highly hydrated polysaccharides which mainly consists of D-galacturonic acid (D-GalA). There

are two fundamental kinds of pectin: homogalacturonan and rhamnogalacturonan I. Homogalacturonans are homopolymers from 1,4-α-D-GalA that contain up to roughly 200 GalA monomers and are approx. 100 nm in length. Furthermore, there are two types of homogalacturonans that are structurally different, xylogalacturonan and rhamnogalacturonan II, with the former being a substituted homogalacturonan, with appendant α-D-Xyl units at the C3-O position of about half of the GalA units and the latter being a complex homogalacturonans with four distinct side groups containing several different kinds of sugar linkages. (Buchanan, Gruissem, and Jones 2015). Table 2 gives an overview on hemicelluloses and pectins.

Table 2: Overview of related data on hemicellulose and pectin (Ragnar et al. 2014).

Polysaccharide	Occurrence	Composition	Properties
Galactogluco-mannan	Cell walls of softwoods	Galactose (15 %), glucose (15 %), mannose (70%); acetylated	Relatively soluble, readily degraded in kraft pulping
Glucomannan	Cell walls of softwoods and (small amounts) hardwoods	Galactose (2 %), glucose (24 %), mannose (74 %); acetylated	Low solubility, readily degraded in kraft pulping
Xylan	Cell walls of hardwoods, monocotyledons and softwoods	Xylose (75 % in softwood, 90 % in hardwood), 4-O-methyl glucuronic acid (17 % in softwood, 10 % in hardwood), arabinose (8 % in softwood); acetylated in hardwood	Soluble in alkali, relatively stable in kraft pulping
Pectin	Middle lamella and outer part of cell walls	Galacturonic acid, rhamnose, arabinose, galactose, apiose, xylose: individual proportions might vary; other sugar may also occur	Degraded in alkali
Xyloglucan	Outer part of cell walls	Glucose (57 %, xylose (30 %), galactose (8 %), fucose (5 %)	Binds specifically to cellulose

Lignin

Woody tissue of plants also incorporate the aromatic polymer lignin, which is synthesized by radical polymerization. Its structure is very complex and incorporates several structural properties, which are unusual for biopolymers: it is crosslinked by various types of ethers and C-C bonds and has no well-defined primary structure. The β-O-4 bond which can be cleaved in chemical pulping, is the most common bond between lignin monomer units. Other bonds such as C-C bonds are more stable than ethers and known as condensed bonds. The ability of lignin to form multiple covalent bonds and noncovalent interactions with polysaccharides enables it to crosslink different polysaccharides in the cell wall. This results in a woody and stiff cell wall with low swelling capability (Ragnar et al. 2014; Rowell 2013).

Extractives and inorganics

Apart from polymeric structure units, low molecular mass compounds are found in plants as well. These molecules can be hydrophilic and water-soluble, such as sugars and phenols, or hydrophobic compounds, e.g. waxes, fats and fatty acids. They do not contribute much to the structure of the plant or the pulp but may cause problems during pulping. Some of these extractives can contribute to the plants color.

Inorganics are mostly silicates and metal salts, where Ca^{2+} is the most common cation. Transition metal ions, such as Fe^{3+} and Mn^{2+} may disturb the bleaching reaction of the pulp (Ragnar et al. 2014; Rowell 2013).

Protein

In plant cells, protein constitute a relatively large part (around 5-10 %) of the dry weight and carry out various essential functions, such as enzyme activity, structural support and cell signaling. The function and solubility are determined by the protein structure (amino acids composition and folding). Depending on the conditions, alkaline pulping degrades disulfide bridges, disrupts hydrogen bonds and (partly) hydrolyses peptide bonds between amino acids, rendering the product soluble. (Florence 1980; Smith and Hansen 1998)

1.2　Chemical pulping and bleaching

The most interesting fraction of *M. spicatum* for utilization in packaging materials is cellulose, which can be separated from the biomass blend structure by mechanical and/or chemical processes, i.e. pulping. The most common chemical pulping processes are the kraft and the sulfite process, which remove residual wood compounds, such as lignin and hemicelluloses.

This work is aimed for establishing very simple pulping methods using soda pulping, which is as in the case of the kraft process conducted at alkaline conditions. This process mainly relies on a hot sodium hydroxide solution, which degrades and solubilizes the polymeric structure of lignin. It is important to optimize the process for the specific type of biomass, since strong alkaline conditions lead to cellulose degradation. This degradation can be limited by addition of additives such as anthraquinone.

For the bleaching process hydrogen peroxide was selected: a chlorine-free, environmentally friendly, strong oxidizing agent. In alkaline conditions, the equilibrium of H_2O_2 shifts to the formation the active species hydrogen peroxide anion (-OOH). The strongly nucleophile reaction of this anion, converts electron-rich chromophores, e.g. unsaturated aldehydes and ketones and phenolic ring-conjugated ethylenic and carbonyl groups to their non-chromophoric counterparts. These reactions of lignin with peroxide are irreversible and lead to a removal of most of the chromophoric groups in the molecule. This process was used for non-wood materials like brewer's spent grain and wheat straw (Mussatto, Rocha, and Roberto 2008; Zhao et al. 2004).

1.3   Biogas

Another possibility to gain value from cellulose-rich biomass such as *M. spicatum* is to convert the energy stored in the polysaccharides into biogas. This is achieved via anaerobic metabolization of microorganism. The resulting biogas such as methane is rich in energy and can be used as fuel for heating and electricity generation. By converting biomass to biogas, the energy-intensive drying process can be avoided, which would be necessary in case of a thermal utilization.

Anaerobic digestion
The decomposition of organic material via microorganisms in absence of oxygen is called anaerobic digestion (AD) and occurs in three steps:

- decomposition of plant or animal matter by bacteria into molecules such as sugars,
- conversion of decomposed matter to organic acids, and
- organic acid conversion to methane gas and CO_2.

This process can be utilized to treat waste material such as bio-solids, livestock manure and wet organic materials in a special digester. In each case, the product of digestion is a combination of gases, generally methane and carbon dioxide as main component. The resulting methane can be used as source for heat and electricity.

Anaerobic processes can occur naturally or in a controlled environment such as in a biogas plant. In a biogas plant, wet organic materials inoculated with various types of bacteria are fermented in an airtight container called a digester. The biogas produced in this manner is typically 55 % - 75 % pure methane, depending on substrate and system design, the rest is mostly CO_2. In municipal waste process systems, the waste is preprocesses (sorted and ground) and then submitted to anaerobic digestion. The excess filtrate is fed back into the system, the remaining solids are further utilized as compost or landfill and the biogas (55 % of which is methane) is collected (Rogoff and Screve 2019).

2. Materials and Methods

2.1 Materials

Chemical (CAS No.)	Purity	Supplier
Acetic acid (64-19-7)	100 %	Carl Roth
Acetone (67-64-1)	≥99.5 %	Carl Roth
D(+)-galactose (59-23-4)	for biochemical purposes	Merck
D(+)-glucose anhydrous (14431-43-7)	for biochemical purposes	Merck
D(+)-mannose (3458-28-4)	for biochemical purposes	Merck
D(+)-xylose (58-86-6)	for biochemical purposes	Merck
Ethanol (64-17-5)	≥99.5 %	Carl Roth
Helium	≥99.999 %	Linde
Hydrochloric acid (7647-01-0)	37 %	Carl Roth
Hydrogen peroxide (7722-84-1)	30 %	Carl Roth
L(-)-fucose (2438-80-4)	for biochemical purposes	Merck
L(+)-arabinose (5328-37-0)	for biochemical purposes	Merck
L(+)-rhamnose (10030-85-0)	for biochemical purposes	Merck
Sodium azide (26628-22-8)	purest	Merck
Sodium chlorite (7758-19-2)	80 %	Sigma-Aldrich
Sodium hydroxide	50 %	Aldrich
Sodium hydroxide (1310-73-2)	≥99 %	Carl Roth
Sulfuric acid (7664-93-9)	96 %	Carl Roth
Toluene (108-88-3)	≥99.5 %	Carl Roth

2.2 Methods

Sample acquisition

Sample material for all analysis was collected by hand in the Old Danube in Vienna, Austria (48°22'13.94''N, 16°43'45.97''E) in late summer 2018. The sample was stored in a freezing room at -15 °C and the required material was thawed at room temperature (RT) a day before use.

Sample preparation

The plant material was ground to the lengths of 0.5 cm as well as 2 cm (Retsch Cutting Mill SM 100). For chemical analysis, parts of the sample were deep-frozen at -80 °C (Sanyo ultra-low temperature freezer) and freeze-dried (Christ Alpha 1-4, LD plus freeze dryer). The dried material was further ground via an ultra-centrifugal mill (Retsch ZM 200 ultra-centrifugal mill) to a maximum size of 0.5 mm. Thereafter the sample was dried again in a vacuum dryer (Goldbrunn 1450 vacuum dryer)

Ash content

The biomass was incinerated at 550 °C for 2 h and the ash content was determined gravimetrically according to TAPPI Test Method *T 211 Om-12.

Extractives content

The biomass was extracted according to TAPPI Test Method T 12 Wd-82 to determine the extractives content:

The first extraction was conducted with toluene/ethanol 2:1 (v/v) as solvent and the second extraction with pure ethanol. Additionally, the sample was washed with hot DI water. The extracted residues were combined and then dissolved in hexane and methanol (1:1), phase-separated and analyzed via H-NMR analysis. Table 3 shows a summary of the samples and their abbreviations.

Table 3: Sample names and definitions

Sample names	Definition
Native sample (0.5 cm)	Native *M. spicatum* ground to a maximum size of 0.5 cm
Native samples (2 cm)	Native *M. spicatum* ground to a maximum size of 2 cm
EF sample	Extractive-free sample, ground to a maximum of 0.5 mm

Chlorite holocellulose

Note: For comparison and GPC analysis the holocellulose was isolated using the chlorite method at just 40 °C instead of 70 °C, to avoid oxidative cellulose degradation.

2.5 g of EF sample were suspended in 80 ml of hot deionized (DI) water. Then 0.5 ml of acetic acid and 1 g of sodium chlorite were added, and the mixture was heated to 70 °C. After 1 h, the same amount of acetic acid and sodium chlorite were added. This cycle was repeated for a total of three additions of acetic acid and chlorite, thereafter the mixture was kept at 70 °C of a total of 24 h reaction time. The crude holocellulose was then washed with water and acetone. After 24 hours of drying in the vacuum-drying oven (Goldbrunn 1450 vacuum dryer) the crude holocellulose weight was determined.

The corrected holocellulose content was determined by subtracting its inorganic (ash), protein and lignin residues content.

The ash content was determined by thermogravimetry (Netzsch TG 209F1 220-10-056-K
) at 650 °C for 2 h, the lignin content by Klason lignin and acid-soluble lignin (Rowell 2013) and the protein content by nitrogen determination via elementary analysis.

Lignin content (acid-insoluble/acid-soluble)

The acid-insoluble lignin was determined gravimetrically. Therefore 0.2 g of EF sample were treated with 72 wt% sulfuric acid for the primary hydrolysis, initially the sample was put on ice and then further hydrolyzed at RT for 2 h. For the secondary hydrolysis, the mixture diluted with DI water to a sulfuric acid concentration of 4 % and was autoclaved at 125 °C for 1 h. The acid insoluble lignin was determined gravimetrically and the acid-soluble lignin via UV/VIS photometry (Perkin Elmer Lambda 35 UV/VIS Spectrometer) at 205 nm and an absorptivity of 110 l / (g cm) (TAPPI Test Method T222 Om-88).

Monosaccharide analysis

Total hydrolysis

For the primary hydrolysis 72.3 % sulfuric acid were used and a sample of holocellulose was stirred for 30 min at 100 RPM and further 3 h at 250 RPM at RT (Rotatherm, Liebig).

The secondary hydrolysis step was carried out for 90 min at 110 °C in 3-4 % sulfuric acid. The samples were then filtered via a syringe filter unit (0.2-0.45 µm) and neutralized with a NaOH solution (0.025 M) (Harris et al. 1985).

Ion chromatography analysis

Stock solution: monosaccharide concentration of 1 g / l and some drops 1 % sodium azide solution were added for conservation. Standard: side components concentration (e.g. arabinose) 1 mg / l and major components concentration (e.g. glucose) 10 mg / l. Columns: CarboPac SA10 precolumn (Dionex), CarboPac SA10 column (Dionex) (Harris et al. 1985).

Methanolysis

1-2 mg of dried sample was treated with 4 ml acidic methanol and heated for 3-5 h at 100 °C. Thereafter 400 µl of anhydrous pyridine were added. Subsequentially 200 µl of sorbitol standard solution (5 mg sorbitol per ml methanol) were added, the solvent was evaporated under a nitrogen stream and the samples then put into a freeze dryer overnight.

Next 200 µl of anhydrous pyridine were added and the samples were incubated at RT for 1 h. Then 200 µl of anhydrous pyridine containing 1.5 mg of 4-Dimethylaminopyridine (DMAP) per ml pyridine were added as well as N,O-Bis(trimethylsilyl)trifluoroacetamide (BSTFA) containing 10 % trimethylsilyl chloride (TMCS). The suspension was then vortexed and heated at 70 °C for 2 h. After a 15 min storage of the samples at -20 °C 800 µl ethyl acetate were added. The test tubes were then centrifuged, and the solution applied to GC-MS via splitless injection (Sundheq et al. 1996).

Amount of uronic acids in holocellulose (carboxyl groups)

0.01 g of sample was weighted into a 20 ml glass tube. The sample was suspended and stirred in 10 ml DI water. Then 1 ml of 0.01 M HCl was added and stirred again for at least 1 h. Thereafter the sample was transferred into the titration vessel, where it was titrated with 0.01 M NaOH while stirred and the conductivity was measured (Metrohm Automated Titration: 800 Dosino, 856 Conductivity Modul, 801 Stirrer).

Heavy metals

As sample preparation, dried samples were weighted into the Xpress Vessel (CEM). 4 blanks and 3 reference samples had to be included in each batch of microwave digestion by adding 4 empty vessels to the samples and weighting 150 mg of 3 certified standard sample materials which were related to the samples into the Xpress Vessels. The samples, reference samples, and blanks were wet out with 3 ml nitric acid (65 %) and left in the hood overnight at RT. Then 6 ml of hydrogen peroxide (30 %) was added to each vessel. The samples were digested for 1.5 hours in a microwave (Mars 6 System, CEM GmbH). Microwave parameters:

- Stages: 1
- Power: 1030-1080W
- Ramp time: 20-25 min
- Hold time: 20 min
- Temperature: 200 °C

After the microwave digestion the samples were analyzed via ICP-OES (Optima 8300 ICP-OES, Perkin Elmer) for their content of the following elements: Ca, Mg, P, S, Cr, Co, Ni, Cu, Zn, Cd, Pb, Fe.

Elementary analysis

According to the SOP "C/H/N-Analyse" of the Faculty of Chemistry, University of Vienna, in short:

2-3 mg of the sample is incinerated at approx. 990 °C (2400 CHN Elemental Analyzer, Perkin Elmer), resulting in a mineralization of the analyte. The gas mixture of CO_2, H_2O and N_2 is then separated by chromatography, detected and quantified by thermal conductivity.

Attenuated total reflection Fourier transform-infrared spectroscopy (ATR-FTIR)

The samples were ground, dried and characterized after by FTIR (Perkin Elmer Frontier Infrared Spectrometer). The IR spectra were measured in the spectral range of 650-4000 cm^{-1} and composed out of 4 sequential measurements. The spectra were base line corrected and normalized.

Nuclear magnetic resonance spectroscopy

All NMR spectra were recorded on a Bruker Avance II 400 (resonance frequencies 400.13 MHz for ^{1}H and 100.63 MHz for ^{13}C) equipped with a 5 mm liquid N_2-cooled cryo-probehead (Prodigy) with z–gradients at room temperature with standard Bruker pulse programs. The samples were dissolved in 0.6 ml of the respective solvent. Chemical shifts are given in ppm, referenced to residual solvent signals (CDCl$_3$: 7.26 ppm for ^{1}H, MeOD: 3.31 ppm for ^{1}H, DMSO: 2.49 ppm for ^{1}H, 39.6 ppm for ^{13}C).

Isolation of macromolecular constituents

Isolation of a protein-rich fraction

The extraction of the protein-rich fraction was conducted according to Harrysson et al. 2018, in short: Native, wet *M. spicatum* (0.5 cm) was suspended in DI water to a 1:6 ratio using an Ultra-Turrax IKA T 10 basic for 2 min. This process was followed up by stirring for 1 h at 8 °C. While keeping the suspension on ice the pH was adjusted to 12 with a NaOH solution (1 M), then the mixture was centrifuged at 9223 RCF for 10 min. The supernatant was decanted, and the pH was adjusted to 2 with HCl (1 M) while the solution was kept on ice. The leftover sediment was collected, vacuum dried for the subsequent extraction of pectin. The supernatant (at pH 2) was frozen at -20 °C overnight, rethawed and then centrifuged at 9223 RCF for 10 min. The pellet was then vacuum dried and analyzed via ATR-FTIR (Perkin Elmer Frontier Infrared Spectrometer) and H-NMR.

Isolation of a lignin-rich fraction

According to Lin 1992, the supernatant and wash of the pulping experiment were collected, neutralized with HCl and evaporated to about a tenth of its original volume. After a second filtration and subsequent centrifugation to remove residual solids, around 25 ml of the supernatant was transferred to a 50 ml centrifuge tube and acidified with HCl (~4 M) to pH 1.5. After 30 min of reaction time precipitation took place and was centrifuged and washed to neutrality. The residue was vacuum-dried overnight. The lignin-rich fraction was then analyzed via ATR-FTIR (Perkin Elmer Frontier Infrared Spectrometer) and H-NMR.

Isolation of a pectin-rich fraction

The extraction of the pectin-rich fraction was conducted according to Harrysson et al. 2018: the remaining insoluble fraction after the isolation of the protein-rich fraction was washed with DI water several times, then suspended in 200 ml of HCl (0.01 M) and stirred at 90 °C for 4 h. After cooling to RT the mixture was centrifuged at 9223 RCF for 10 min. The supernatant was separated and freeze-dried, the insoluble fraction was kept for potential further extractions.

Pulping and bleaching experiments

Pulping experiments

To the native sample (2 cm) a NaOH solution (0.5 M) was added (liquid to dry matter ratio of 20). Thereafter the suspension was heated to 80 °C and stirred for 4 h. After this process the mixture was filtered (approx. 30-40 µm cellulose cloth) and the residue washed with DI water until a pH of 8-9 was reached. Then the pulp was either stored wet in the fridge at 8 °C, i.e. never-dried pulp for papermaking or dried in the vacuum dryer for further analysis.

Pulping/bleaching experiments

To the native sample (2 cm) a NaOH solution (0.5 M) was added (liquid to dry matter ratio of 20). Thereafter the suspension was heated to 80 °C, 3 % w/w hydrogen peroxide solution was added, and the mixture was stirred for 4 h. Then the mixture was filtered (approx. 30-40 µm cellulose cloth) and the residue washed with DI water until a pH of 8-9 was reached. Then the pulp was either stored wet in the fridge at 8 °C, i.e. never-dried pulp for papermaking or dried in the vacuum dryer for further analysis.

Further conducted pulping/bleaching experiments

In order to find the pulping and/or bleaching experiments that would yield the best mechanical properties, many different setups were tested (Table 1). The source material and its amount, pulping chemicals, complexing agents and catalysts were varied, as well as temperature, duration of heating and liquid to biomass ratio (LTBR). The native source material already contained around 90 % of water, thus, to achieve the LTBRs lower than 10, the biomass was concentrated via a hand-operated press. The lowest possible solid content then was approx. 30 %. All pulping experiments were conducted according to standard pulping/bleaching experiments (see above), the pulping chemicals used, temperature, durations and liquid to biomass ratios (LTBRs) were adjusted for each experiment according to Table 4.

Table 4: A selection of various puling/bleaching experiments conducted

Source material	Amount of source material, dry [g]	Chemicals	Temperature [°C]	Duration [h]	Liquid to biomass ratio (LTBR)
Native *M.spicatum*	2, 4, 8	NaOH 0.5 M	80	2, 4, 6, 21	20
Native *M.spicatum*	2, 4	NaOH 0.5 M	80	4	5, 6, 7, 10, 15, 20
Native *M.spicatum*	2, 4	Na_2CO_3 0.1 M	80	4	20
Native *M.spicatum*	2, 4	KOH 0.5 M	80	4	20
EF	2, 4	NaOH 0.5 M	80	4	20
Native *M.spicatum*	4, 8, 100	NaOH 0.5 M, H_2O_2 3 wt%	80	4	20
Native *M.spicatum*	2, 4	Na_2CO_3 0.1 M, H_2O_2 3 wt%	80	4	20
NaOH pulp (4h)	2	NaOH 0.5 M, H_2O_2 3 wt%	80	4	20
NaOH pulp (4h)	2	H_2O_2 3 wt%	80	4	20
NaOH pulp (4h)	2	NaOH 0.5 M, H_2O_2 3 wt%,	80	4	20
NaOH pulp (4h)	2	NaOH 0.5 M, H_2O_2 3 wt%, EDTA/$MgSO_4$ 0.3 wt%	80	4	20
EF	2	NaOH 0.5 M, H_2O_2 3 wt%	80	4	20

Papermaking and testing

Papermaking

About 0.509 g (dry weight) of pulp, which corresponds to a circular standard paper (9 cm diameter, cm, 80 g / m^2), were suspend in approx. 30 ml of DI water and were fibrillated with an IKA Ultra-Turrax T 10 basic at 30,000 RPM for 1 min. Then 200-300 ml of DI water were added to the suspension. The suspension was concentrated by vacuum filtration in a Büchner funnel through two combined and prewetted filter papers (pore size: approx. 12 μm). After being sufficiently dry, the filter cake with still attached filter was pressed in-between two laminated papers in a Frank PTI, Rapid-Köthen sheet former for 10 min at 92 °C, and a vacuum pressure of 80 mbar. The resulting paper samples were then subjected to tensile strength tests and microscopy.

Paper testing

Before testing, the paper samples were conditioned for 24 h at 21 °C and 45 % relative humidity. The paper samples (circular shape, 9 cm diameter) were cut into 6 strips of 6 cm x 1 cm dimensions. Of these strips the thickness was measured on 5 different spots via a paper thickness gauge and their mass was determined gravimetrically. Then the sample was clamped into the Zwick Roell Z20 tensile strength testing machine equipped with a 500 N load cell. The measurements were conducted at a displacement rate of 1 mm min^{-1}.

Biogas experiments

Degradation kinetics

From around 3.2 kg of thawed native material, sample bags were prepared to put into the inoculum according to their projected degradation after 1, 3, 7, 10, 20 and 40 days. For each day 3 determinations were conducted (A, B, C). Bags A+B (Ankom R1020 Forage Bags 10x20 cm) were used for the degradation kinetics and bags C were used for papermaking experiments. The bags were then submerged in the inoculum. After the degradation, samples A+B were washed until the wash water was clear, dried at 40 °C and then analyzed. Samples C were resuspended in DI water treated with sodium azide (0.001 wt%) for conservation. From the samples C papers were made and the samples A+B were weighted and analyzed further.

Bio-methane potential

Sample material and inoculum (1:3, dry matter) were fermented at a constant temperature of 37.5 °C. Cellulose was used as a reference for microbial activity. The methane and carbon dioxide concentration were determined via the portable gas analyzer Dräger X-am 7000, which was calibrated with a calibration gas (50 % CH_4, 50 % CO_2).

Calculation of the results

Firstly, the yielded gas volumes had to be related to 273 K and 1013 hPa atmospheric pressure, i.e. norm liter [l_N] of the dry gas, and water vapor was subtracted. Therefore, before each measurement gas temperature (equaled RT) and atmospheric pressure had to be documented. Equation 1 shows the corresponding relationship.

$$V_0^{tr} = V \cdot \frac{(p - p_w) \cdot T_0}{p_0 T}$$

V_0^{tr}	Volume of the dry gas in normal conditions [mlN]
V	Gauge of the gas volume [ml]
p	Pressure of the gas phase at time of gauging [hPa]
pw	Vapor pressure at current RT [hPa]
T_0	Norm temperature; T_0 = 273 K
p_0	Norm pressure; p_0 = 1013 hPa
T	Temperature of the gas (equals RT) [K]

To calculate the volumetric methane, yield the major components of the biogas (methane and carbon dioxide), their volumetric amount in % had to be determined (Equation 2).

$$C_{korr}^{tr} = C_{CH_4(CO_2)} \cdot \frac{100}{C_{CH_4} + C_{CO_2}}$$

C_{korr}^{tr} :   corrected concentration of biogas components in the dry gas [vol%]

$C_{CH_4(CO_2)}$: determined concentration of methane (or carbon dioxide) in the gas [vol%]

C_{CH_4}:   determined concentration of methane in the gas [vol%]

C_{CO_2} :   determined concentration of carbon dioxide in the gas [vol%]

To determine the biogas that was produced solely via the biomass, the gas production of the inoculum had to be subtracted from the total gas volume produced. Therefore, the gas volume of the inoculum had to be determined (Equation 3) and subtracted from the total gas volume.

$$V_{IS(korr.)} = \frac{\sum V_{IS} \cdot m_{IS}}{m_M}$$

$V_{IS(korr.)}$	Gas volume produced by the inoculum [mlN]
$\sum V_{IS}$	Sum of gas volume of the analysis including the gas volume of the inoculum for the test duration [mlN]
m_{IS}	Mass of the inoculum for the analysis [g]
m_M	Mass of the inoculum used as reference [g]

To make the gas volume comparable, it was related to the organic dry matter amount [lN kg^{-1} ODM] (Equation 4). Hence the determined value is free of water and ash content and comparable to other measurements.

Equation 4: Calculation of the specific biogas yield in relation to ODM

$$V_S = \frac{\sum V_n \cdot 10^4}{m \cdot w_T \cdot w_V}$$

V_S Specific biogas yield in relation to ODM [$l_N \cdot kg^{-1}$ ODM]

$\sum V_n$ Net gas volume [mlN]

m Mass of the weighted substrate [g]

w_T Dry matter content of substrate [%]

w_V Organic dry matter content of substrate [%]

3.   Results and Discussion

3.1   Chemical Composition of *Myriophyllum spicatum*

Since the number of recent publications surrounding the chemical composition of *Myriophyllum spicatum* is still very limited, we investigated the plant's composition first, which was essential to evaluate the potential of *M. spicatum* as cellulose source and design respective pulping processes. We conducted a chemical analysis to determine its content of holocellulose, lignin, extractives, protein and ash (as shown in Figure 4).
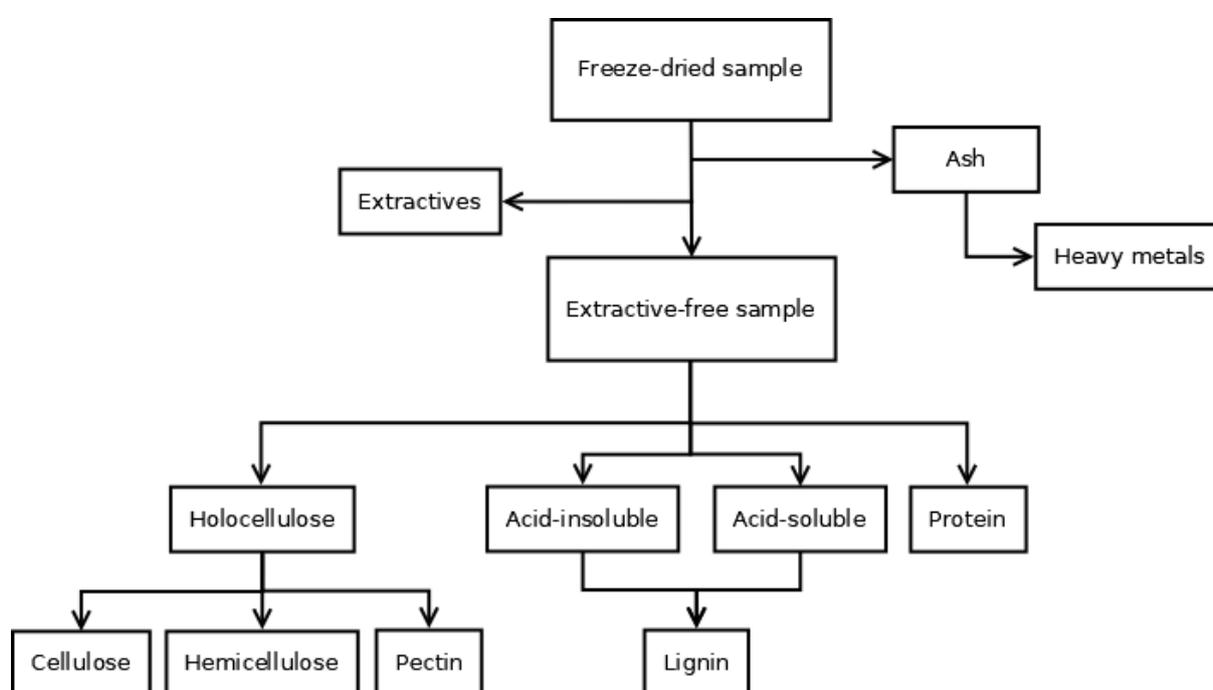
Figure 4: Flowchart of the chemical composition analysis of M. spicatum.

Ash and heavy metals

The ash content, which was determined gravimetrically, amounted to 11.6 ± 0.1 %. To further analyze the non-volatile residue a heavy metal analysis was performed to get an overview of some of the potential health risks if the plant was used as packaging material. The detected amounts of heavy metals are summarized in Table 5.

Table 5: Heavy metal analysis results of M. spicatum

Element	Ca	Mg	P	S	Cr	Co	Ni	Cu	Zn	Cd	Pb	Fe
Average (mg/kg)	26,800	6,000	1,120	2,340	4.18	n.d.	5.5	6.27	32	n.d.	1.68	356.1
SD (mg/g)	0.5	0.18	0.01	0.05	0.06	n.d.	0.1	0.79	0.4	n.d.	0.1	20.5

Some metal ions, such as Fe^{3+} and Mn^{2+} can exert an inhibitory influence on the bleaching efforts, thus several strategies such as complexation with EDTA have been tested during our research, but no significant visual improvement on the bleaching result was observed.

The effect of phytoaccumulation of aquatic plants is well-known and thoroughly studied (Keskinkan et al. 2004; Rıdvan Sivaci, Sivaci, and Sökmen 2004; Stanley 1974). If, therefore, any successful strategy involving *M. spicatum* for food packaging purposes was to be developed, one must be aware of the upper limits that were set by the Council of Europe, which assumes 100 % migration to food stuffs: e.g. 2 µg/dm² of cadmium and 3 µg/dm² of lead. A hypothetical standard paper (80 g/m²) of native *M. spicatum* would amount to 1.34 µg/dm² of lead. This value would be well below the upper limit, especially considering that a necessary pulping process would further reduce the amount of heavy metals present in the material ("Council of Europe - Resolution Ap on Paper and Board Materials and Articles Intended to Come into Contact with Food Stuffs, 2002").

The same goes for attempts to process the plant for foodstuffs, assuming that the hurdle of novel food regulation could be overcome (which would take effect if the food or food ingredient had no history of 'significant' consumption in the EU prior to 15 May 1997). According to the Commission Regulation of the EU (COMMISSION REGULATION (EC) No 1881/2006) the maximum amount of cadmium and lead in leaf vegetables is set to 0.1 and 0.05 mg/kg wet weight, respectively. Hence, fresh *M. spicatum* from the Danube which has a dry matter content of around 10 %, contained 340 % of the maximum levels of lead set by the EU and therefore, would not be safe for consumption. Even if the plant was used just as an ingredient or flavor heavy metal upper limits could be reached unintentionally.

Extractives

The residual extractives were removed by a two-stated Soxhlet extraction, first with Tol/EtOH (ratio 2:1) and finally with pure EtOH. The amount of extract was of 15.4 ±0.1 %, 15.2 ±<0.1 % for the Tol/EtOH fraction and 0.21 ±0.1 % for the EtOH fraction.

Due the relatively high protein content (compare with 'protein' section), a possible, unwanted coextraction of some amount of protein with EtOH could not be excluded, thus potentially leading to an artificially higher extractives amount.

The extract of the Tol/EtOH fraction was subsequently dissolved in the immiscible solvents methanol and hexane. The resulting two fractions of the extract (MeOH and hexane fraction) were dried and finally analyzed via H-NMR in MeOD and $CDCl_3$. The spectra were very similar and showed mainly fatty acids, but the hexane-extracted sample showed more intense peaks (Figure 5). The most prominent signals were the peaks of terminal methyl groups (A) and of hydrogens at saturated (B, D) and unsaturated methylene groups (G) in fatty acids.
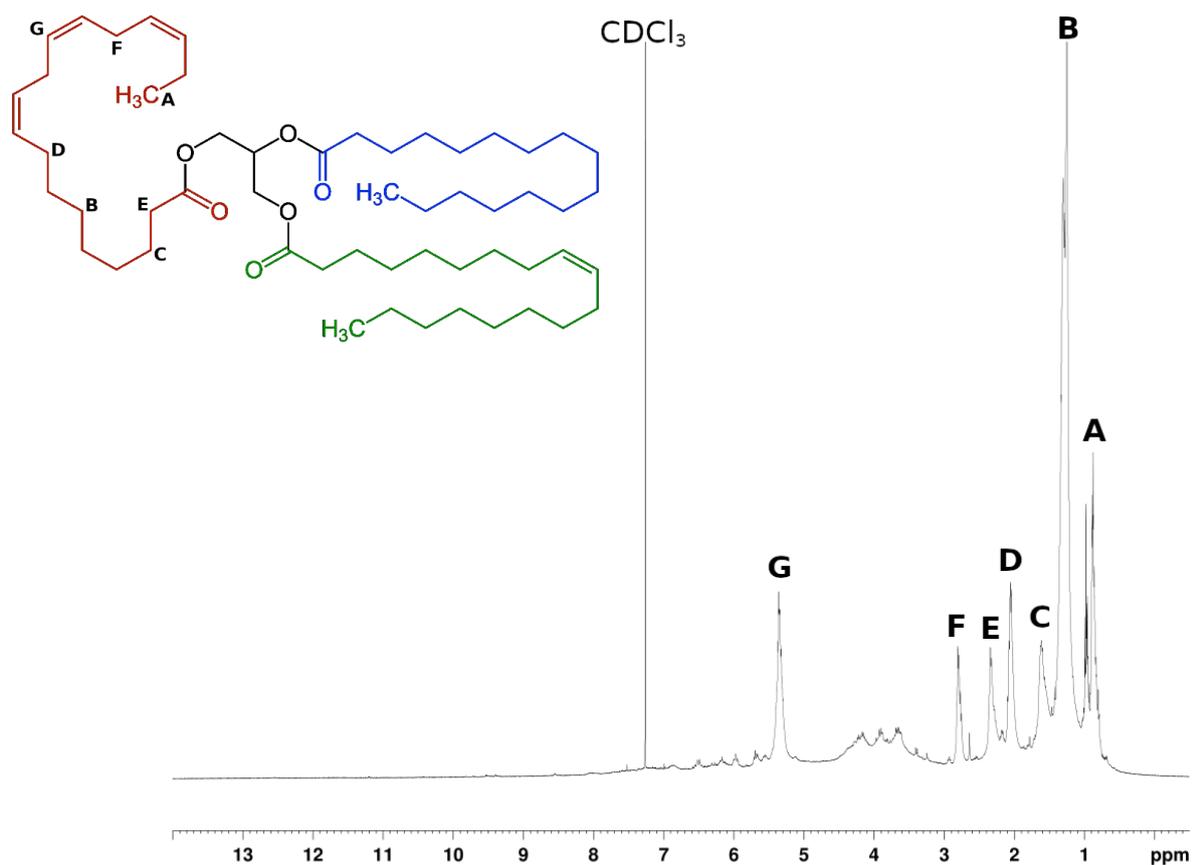
Figure 5: H-NMR spectrum of hexane-extracted M. spicatum extractives including an illustration of the hydrogen peaks allocation on a triglyceride.

To obtain more information of the extract composition, it is necessary to separate each fraction further, e.g. by HPTLC before conducting analyses via NMR or mass spectrometry. These experiments could not be carried out in the framework of this master's thesis but are planned for follow-up studies. More information about the composition would be important for the development of a biorefinery approach based on *M. spicatum*. In the literature it was shown that M. spicatum released ellagic, gallic and pyrogallic acids and (+)-catechin and allelopathic polyphenols inhibiting the growth of freshwater cyanobacteria *Microcystis aeruginosa* (Nakai 2000), these molecules are just one example for valuable fractions which could be extracted from the plant.

Protein

As the next macromolecular constituent of the plant, the protein fraction was analyzed. The amount of protein present in the *M. spicatum* was determined by elementary analysis from the total nitrogen content of 1.93 ±0.10 %.

Similar to the standard method Kjeldahl digestion, a conversion factor was used to relate the total nitrogen content to the crude protein content. The standard conversion factor that is commonly used in the absence of any published factors is 6.25, thus the crude protein content amounted to 12.1 ±0.6 %. This value is called crude protein, because non-protein nitrogen like ammonia, urea and nitrate/nitrite are detected as well and could, if present in the sample, lead to an artificially higher protein content. The conversion factor also brings in a certain inaccuracy, because it is derived from the amino acid composition of the respective protein. Thus, the standard conversion factor had to be chosen for this work (Van Alfen 2014).

Furthermore, a protein-rich fraction was extracted according to Harrysson et al. 2018 by a pH shift and freeze concentration and analyzed by ATR-FTIR.

The comparison of the ATR-FTIR spectra of native *M. spicatum* and the protein-rich fraction (Figure 6) shows that especially the absorption bands at wavenumbers 1600-1750 cm^{-1}, 1500-1520 cm^{-1} and 1100-1350 cm^{-1} are significantly enriched. The 1600-1750 cm^{-1} area represents the C=O (from carboxylic and amide bonds) as well as C-N bonds, around 1500 cm^{-1} aromatic C=C bonds can be observed. The high intensity of the phenol band (1200 cm^{-1}) suggests that this fraction consists of further polyphenolic fractions other than tyrosine, e.g. polyphenols or lignin.

Additionally, the high intensity of the CH_2-related stretching bands in the range of 2925 to 2850 cm^{-1} could be an indication of the presence of fatty acids. (Fasoli et al. 2016).
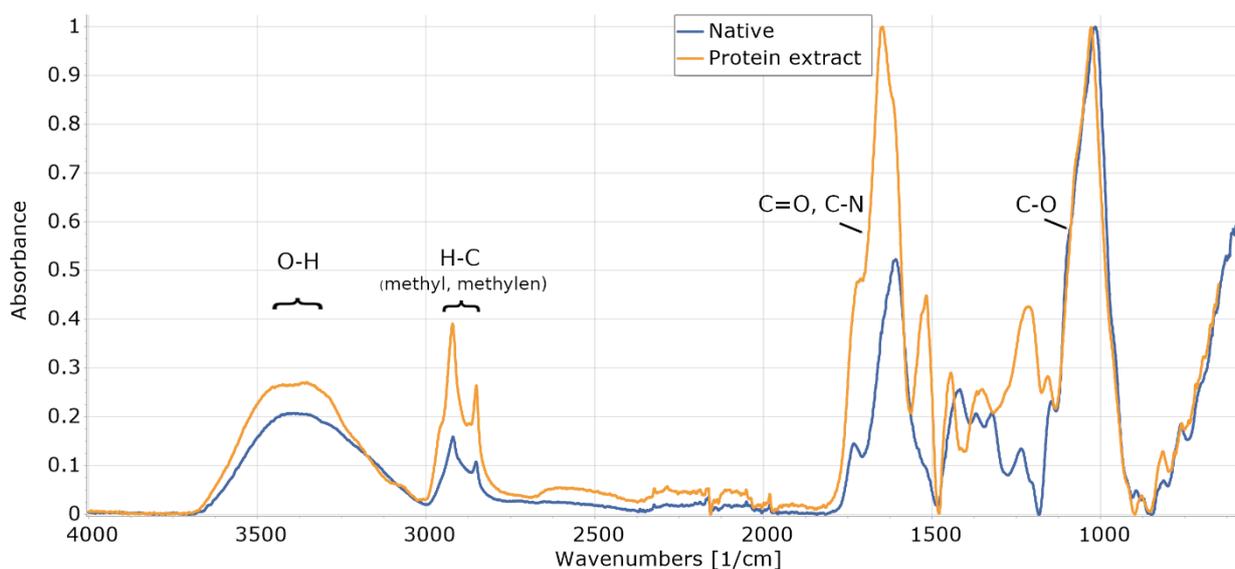

Figure 6: Comparison of ATR-FTIR spectra of native M. spicatum and the protein-rich fraction.

To further analyze this fraction, H-NMR in H_2O and D_2O analysis of the protein-rich sample was carried out. Unfortunately, even at the high concentration of 33 mg/ml the obtained spectrum consisted of broad, overlapped peaks and was not interpretable due to the low solubility of this fraction.

Lignin

The small amount of recent literature available suggested that *M. spicatum* had a certain level of lignin (Marko et al. 2008), hence Klason lignin or acid-insoluble lignin as well as acid-soluble lignin was determined according to Rowell 2013. The Klason lignin analysis yielded 8.56 ±0.15 %, while the acid-soluble lignin amounted to 4.87 ±0.25 %, totaling to 13.4 ±0.4 % of crude lignin. Samples with a relatively high amount of protein could yield an artificially high Klason lignin value, due to condensation reactions (Rowell 2013), thus, the nitrogen content of the

acid-insoluble residue was determined via CHN analysis. The protein content of the acid-insoluble lignin amounted to 30.0 ±0.7 %. In subtracting this value from the crude lignin content, the total lignin content amounted to 10.9 ±1.1 %.

To further characterize the lignin structure, it was precipitated after soda pulping: the pulping liquid was neutralized and concentrated to a tenth of its original volume. Then the pH was adjusted to 1.5 and the resulting precipitate was collected (Lin 1992). As shown in the IR spectrum in Figure 7, the precipitate that did not resemble conventional lignin structures. The spectrum of the extract further indicated that, due to the prominent absorption band at the wavelength 1600-1750 cm^{-1}, considerable amounts of protein had likely been acquired instead (Fasoli et al. 2016).
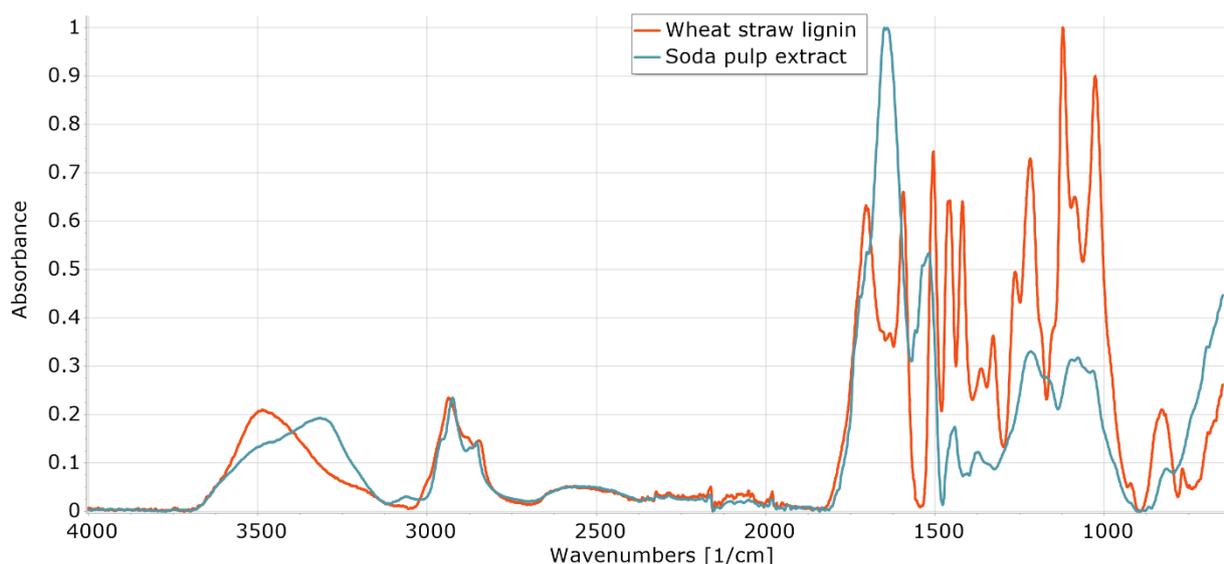

Figure 7: Comparison of ATR-FTIR spectra of wheat straw lignin and soda pulp extract of M. spicatum.

Holocellulose

The group of macromolecules that was of main interest was holocellulose and separated via the chlorite method. In this method, amounts of lignin and protein are decomposed in an oxidative process at acidic conditions (Kantouch, Hebeish, and El-Rafie 1970). The holocellulose was then further analyzed by ATR-FTIR. The sugar composition of the holocellulose was analyzed by total hydrolysis coupled with ion exchange chromatography as well as methanolysis followed by GC-MS.

The chlorite method yielded 51.2 ±0.4 % of crude holocellulose. To take into consideration the residuals of inorganic matter, proteins and lignin; the ash content, nitrogen and lignin content were determined and subtracted from the crude amount leading to a final holocellulose value of 43.6 ±1.4 %. The relatively high standard deviation can therefore be explained by the five-part determination leading to an accumulation of determination errors.

Figure 8 compares the IR spectra of holocellulose and native *M. spicatum*.
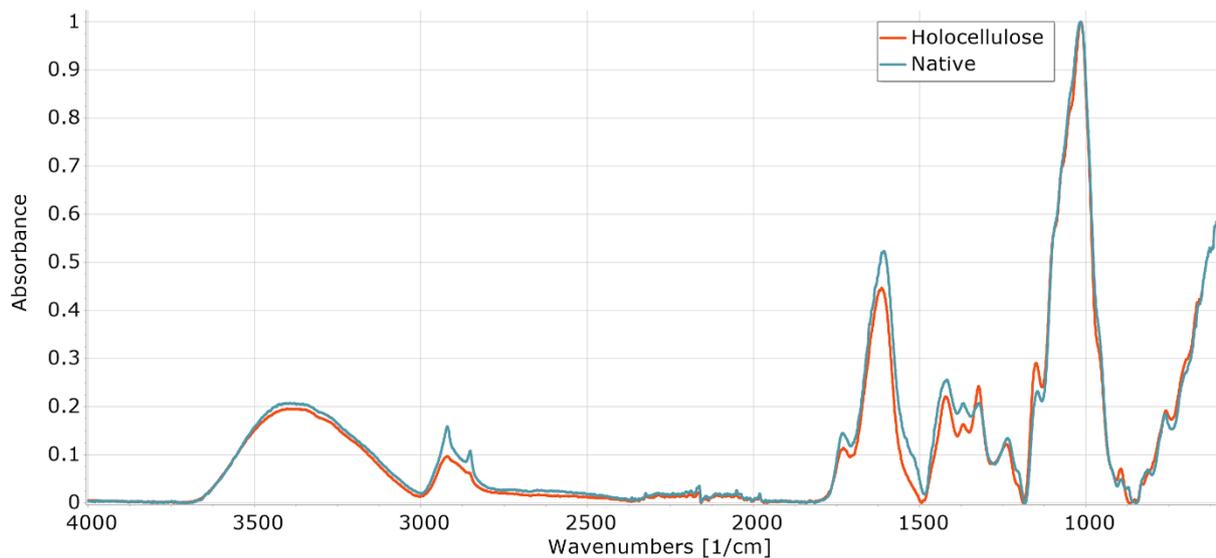
Figure 8: ATR-FTIR spectra comparison of holocellulose and native sample.

The two spectra look rather similar with reductions at the methylene absorption bands (2850 cm^{-1} and 2925 cm^{-1}) representing predominantly the extractives. The carboxylic and amide related bands are also decreased (1600-1690 cm^{-1}) suggesting a reduction in protein content. In addition, intensity of bands at approx. 1400 cm^{-1} and at 1150 cm^{-1} were reduced as well (Fasoli et al. 2016).

After extracting the holocellulose, analyzing its monosaccharide composition was the next goal. However, the results of the monomeric composition obtained via acid hydrolysis followed by IEX chromatography (Table 6), showed that there are also other components than the standard monomeric sugars: only a total amount of 49 % of the hydrolyzed holocellulose could be analyzed with this technique consisting of 41 % of glucose and 8 % of remaining sugars, which are building blocks of hemicellulose and pectin.

Table 6: Total hydrolysis and IEX analysis of holocellulose (prepared at 40°C).

Sugars	Average [%]	SD [%]
Glucose	41.40	0.13
Xylose	2.43	0.06
Mannose	1.77	<0.01
Arabinose	1.57	<0.01
Rhamnose	0.56	<0.01
Galactose	1.65	<0.01
Total	49.4	0.18

But more than 50 % of the holocellulose is unaccounted for and that is, in part, due to the degradation effects of labile compounds like uronic (and hexenuronic) acids by the harsh treatment of the sulfuric acid hydrolysis (Sundheq et al. 1996).

In order to circumvent this problem and to verify the thesis of having a large amount of uronic acids present in the sample, methanolysis followed by GC-MS analysis was used as method. The acid hydrolysis in this case is less severe and enables the detection of uronic acids, crystalline cellulose on the other hand will not be hydrolyzed and thus not be detected (Sundheq et al. 1996).

The results of the methanolysis (Table 7) show large amounts of uronic acids in the holocellulose, suggesting in turn high amounts of pectin, which is constituted mainly of galacturonic acid (HG, RG-I, RG-II) as well as rhamnose (RG-I, RG-II) and other sugars (RG-II) (Buchanan, Gruissem, and Jones 2015).

In order to obtain more information on the amount of galacturonic acid a carboxyl group determination via conductometric titration with 0.01 M NaOH was conducted. It resulted in a comparably high amount of carboxyl groups: 1.35 ±0.04 mmol of free carboxyl groups per g of native sample and 1.40 ±0.04 mmol per g of holocellulose. These rather high values are due to the afore mentioned high availability of pectin, which consist mainly of galacturonic acid, thus providing plenty of carboxyl groups. Additionally, protein could contribute some carboxylic acid groups, since glutamine and asparagine carry carboxylic side groups, therefore the holocellulose carboxy group titration value could be considered the more accurate of the two. Since the sugar compositions of cellulose, hemicellulose and pectin are partly overlapping and the exact monosaccharide distribution in the polysaccharides of *M. spicatum* is yet unknown, a clear assignment of the relative amounts of the various sugars could not be made. Still an estimation of the macromolecular constituents could be deducted: The glucose content of 41.4 % can roughly be attributed to be cellulose, of which at approx. 50 % was amorphous (21.8 % glucose of methanolysis). While hemicellulose, which is represented by the sugars xylose, galactose, arabinose and mannose could be estimated to around 7.4 %. Pectin then, is indicated by the presence of galacturonic acid and rhamnose (the former contributing the large

gap in the total hydrolysis recovery) and amounted to 27.8 %. The rest could be linked to residual amounts of non-standard polysaccharides and sugars, lignin, salts as well as residual protein. The summarized results of the macromolecular components of *M. spicatum* can be found in Table 8.

Furthermore, when comparing the methanolysis results of holocellulose which was isolated by the chlorite method at 40 °C to holocellulose isolated at 70 °C (which is the standard method for wood (Rowell 2013)), a different result in monosaccharide composition could be observed. The most significant differences lay in the glucose and galacturonic acid content. Interestingly, hemicellulose was less prone to hydrolyzation at the higher temperature, which is signalized by the increase of xylose from 1.5 % to 3.2 %. The amount of pectin on the other hand decreased, most likely due to the slightly acidic conditions, signified by the decrease of galacturonic acid from 10.3 % to 14.7 %.

Table 7: Methanolysis and GC-MS analysis of holocellulose, prepared at 40 °C and 70 °C. Values in the table are mass percentages.

Monosaccharides	Holocellulose (40 °C)		Holocellulose (70 °C)	
	Average [%]	SD [%]	Average [%]	SD [%]
Arabinose	1.45	0.07	1.05	0.05
Rhamnose	0.88	0.04	1.13	0.02
Fucose	0.31	0.01	0.52	0.02
Xylose	1.55	0.12	3.20	0.21
Galacturonic acid	10.30	0.28	14.69	0.98
Mannose	0.69	0.01	0.88	0.05
Galactose	1.50	0.05	1.74	0.02
Glucose	21.82	0.33	6.63	1.34

Similar to protein, a pectin-rich fraction was extracted using 0.01 M HCl and analyzed by ATR-FTIR (Figure 9). Compared to the native sample, the pectin-rich fraction showed a significant increase at the band around 1740 cm^{-1}, which could be assigned to the C=O stretching of protonated or methylated carboxylic groups. Thus, displaying a large decrease at the carboxylate and amid bond area (1600-1720 cm^{-1}), which is amplified additionally by the separation of protein via the extraction process.

Furthermore, a decrease of the extractives could be observed (2850-2925 cm^{-1}), indicating their low solubility in a polar and acidic environment (Fasoli et al. 2016).

Further analysis by NMR was not possible due to the low solubility of this pectin-rich fraction.
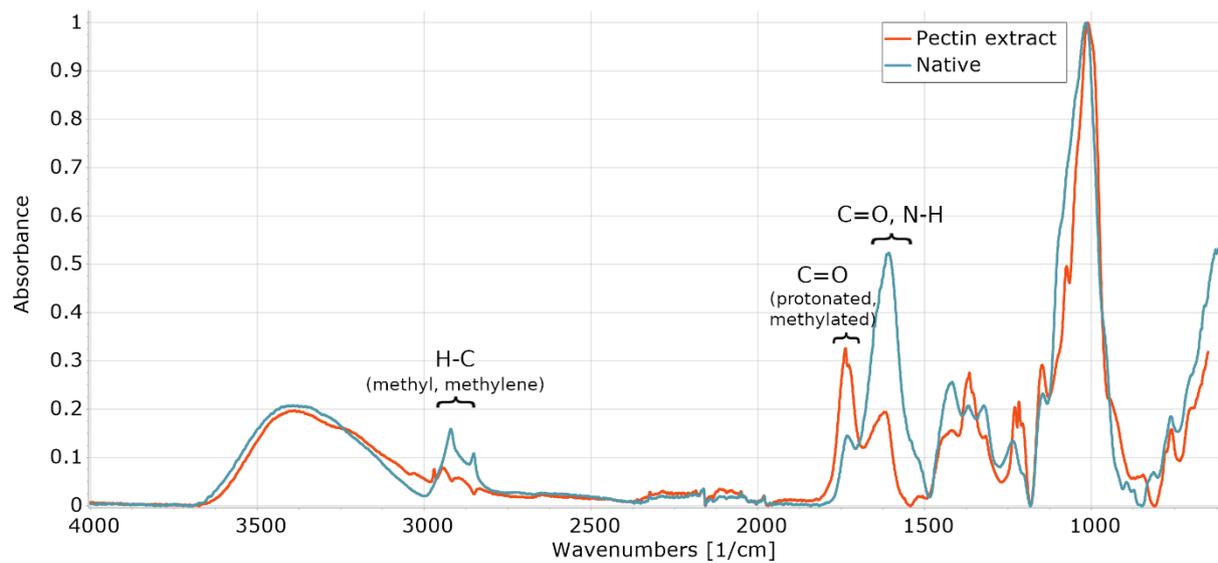
Figure 9: Comparison of ATR-FTIR analysis of pectin extract and native sample.

The 'wet' chemical analysis of the macromolecular constituents of *M. spicatum* resulted to 93.6 %, thus being off the 100 % mark and explaining the 6.4 % of 'other' in Table 8. It is suggested, that this is, in part, due to the mono-, di- and oligosaccharides that were washed out after the extraction with Tol/EtOH as well as cellulose degradation by the chlorite oxidation (Mortha et al. 2015).

Table 8: Summary of the chemical analysis of the components of M. spicatum and the amounts of holocellulose constituents. Values are based on dry matter.

Main component	Component	*M. spicatum* (native)		*M. spicatum* (holocellulose)	
		Amount [%]	SD [%]	Amount [%]	SD [%]
Holocellulose		43.6	1.4	84.1	
	Cellulose	18.1	<0.1	41.4	0.1
	Pectin	12.1	0.6	27.8	1.4
	Hemicellulose	3.2	<0.1	7.4	0.1
Extractives		15.4	0.1		
Lignin		10.9	1.1	4.0	0.2
	Acid-insoluble lignin	6.0	0.1	2.7	0.1
	Acid-soluble lignin	4.9	0.2	1.3	0.1
Protein		12.1	0.6	6.5	0.4
Ash		11.6	0.1	5.4	0.2
Other		6.4		7.5	

Also, at this point, it is important to stretch the notion that these values are not absolute. These analysis', despite being very sensitive (mostly gravimetric) and conducted with utmost care, were developed to analyze mostly wood-derived cellulose fractions. The different species and amounts of components, mostly related to the protein fraction and carbohydrate composition, made the analysis a challenge. On the one hand, these rather unusual carbohydrate compositions as well as the high amount of protein could have caused side-reaction during chlorite oxidation or acidic hydrolysis (this would have affected, among others, the analyzed amount of lignin and sugars). On the other hand, the monomeric sugars were embedded into a very different sample matrix; which could have affected the reliability of the used standard protocols, e.g. in the silanization prior to GC-MS analysis.

It has been demonstrated by the variation of temperature in the holocellulose determination and its effect on the sugar composition, that there is a need for a dedicated non-wood standard analysis protocol.

Taking this into account, the main components were determined in a manner, which was as reliable as possible; but it is certain that there is room for improvement in follow-up research efforts.

With the major macromolecular constituents of *M. spicatum* identified as well as quantified, the initial aim was to process the native plant into a packaging material. The goal was seemingly clear cut: removing mostly lignin, extractives and protein from the plant, while keeping as much of cellulose, hemicellulose and pectin as possible. Preferably, this should be achieved without lowering the degree of polymerization or the crystallinity of the cellulose.

In each pulping project this poses a balancing act, because it is challenging to get rid of the one part of the complex plant structure while keeping the other unharmed (Ragnar et al. 2014). Thus, many different pulping as well as bleaching experiments have been tested and optimized by comparing different (pre-)treatments, the influence of the treatment severity (duration and temperature) and changing the liquid to biomass ratios. A selection of the studied pulping experiments is shown in Table 4 in the '2. Materials and methods' section.

Since measuring the physical properties of papers is a rather time-consuming effort, an effective method had to be established, to determine which pulp would be tested and which would be discarded. The preselection of pulps that were going to be tested for their tensile strength was conducted as follows: The pulps were evaluated according to their visual fibrillation. Pulping attempts that did visually fail to swell the fibers and efficiently remove extractives according to the color intensity of the pulping liquor were not further pursued. Furthermore, their ATR-FTIR spectra were analyzed to estimate the amount of residual protein, which is related to the band intensity in the region of 1600-1750 cm^{-1}. The selected pulps were then formed into standard papers of 9 cm in diameter and a grammage of 80 g/m^2. Of these samples, the most promising two pulps were selected for further chemical analysis: a soda pulp and bleached variant (Table 9). The former was chosen to solubilize protein and lignin, while the latter additionally oxidized the lignin structure and coloring molecules.

Table 9: List of pulping procedures that were selected for further chemical analysis.

Source material	Chemicals	Temperature [°C]	Duration [h]	Liquid to biomass ratio (LTBR)	Yields [%]
Native *M.spicatum*	NaOH 0.5 M	80	2, 4, 6, 21	20	50 ± 6
Native *M.spicatum*	NaOH 0.5 M, H$_2$O$_2$ 3 wt%	80	4	20	34 ± 9

3.2   Chemical characterization of H_2O_2 and NaOH pulps

Ash

The ash content was analyzed by TGA and yielded 8.1 ±0.1 % for the NaOH pulp and 8.0 ±<0.1 % for the H_2O_2 pulp, which is 30 % and 31 % respectively lower compared to the native sample. A lower ash content was to be expected due to the cooking and drying processes.

Extractives

The extraction via Soxhlet with just Tol/EtOH (2:1) totaled to an extractive amount of 7.4 ±0.1 % for the NaOH pulp and 7.2 ±0.1 % for the bleach variant. Thus, the pulping process lead to a reduction of 52 % and 53 % respectively.

Protein

Again, the crude protein content was determined by elementary analysis. This resulted in a total nitrogen content of 0.65 ±0.03 % which, by introducing the standard conversion factor of 6.25 amounted to 4.1 ±0.2 % crude protein content for the NaOH pulp. Thus, the pulping process reduced its crude protein content to a third of the native plant material (12.1 ±0.6 %). The H_2O_2 pulps showed similar results with a nitrogen content of 0.69 ±0.05 % and thus, a crude protein content of 4.3 ±0.3 %.

Figure 10 shows the ATR-FTIR spectra of the native sample compared to the soda pulp for 4 h and 21 h respectively. The carboxylic and amide bond area at 1600-1750 cm^{-1} shows a strong relation between pulping duration and protein content. The longer the pulping process the more protein got solubilized, most likely due to a combination of protein degradation and unfolding of the protein's tertiary and quaternary structures in the alkaline conditions.
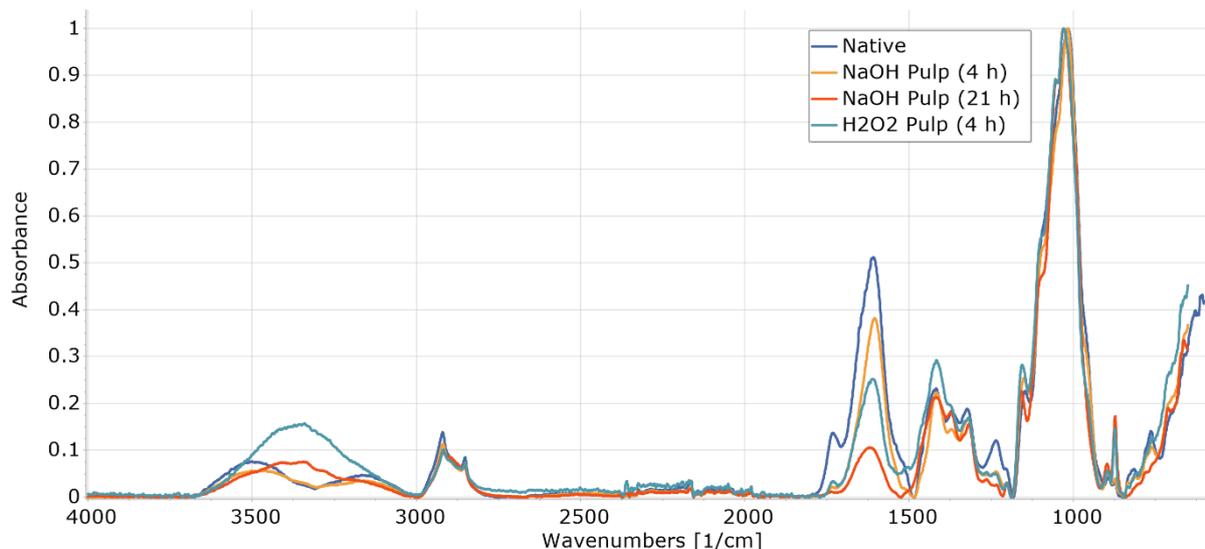

Figure 10: Comparison of the ATR-FTIR spectra of native M. spicatum, soda pulp (4 h and 21 h) and H_2O_2 pulp (4 h).

Lignin

The Klason and acid-soluble lignin analysis yielded 4.0 ±0.3 % of acid-soluble and 13.3 ±0.2 % of acid-insoluble lignin, totaling to a lignin content of 17.3 ±0.2 % for the NaOH pulp. In contrast, analysis of the H_2O_2 pulp gave 4.3 ±0.3 % of acid-soluble and 6.9 ±0.2 % of acid-insoluble lignin (total lignin content of 11.2 ±0.3 %). Thus, the NaOH process lead to an increase of lignin to a content of 59 % (in comparison to the native biomass), while the H_2O_2 process increased the amount of lignin only by 3 %. Since the protein content was reduced to a third of its original amount and proteins were presumably structurally weakened, the condensed protein error was neglected for this analysis.

This significant increase in lignin content suggests the formation of pseudo-lignin, which is composed of carbohydrate and lignin degradation products (Shinde et al. 2018). In addition, one should consider that also protein-induced side-reactions could cause the formation of pseudo-lignin.

Holocellulose

The weight percentage of polysaccharides in Table 10 was estimated from the total sample mass subtracted by the amounts of ash, protein and lignin. The NaOH pulp featured an amount of 63.1 % and the H_2O_2 pulp one of 69.1 %. In comparison, the determined holocellulose of NaOH and H_2O_2 pulp using the chlorite method amounted to 49.3 ±1.29 % and 32.7 ±3.9 % respectively. This constitutes an increase in holocellulose in the NaOH pulp (+13 %) and a significant loss in the H_2O_2 pulp (-25 %) compared to the native sample.

The large difference in the polysaccharide amount can be reasoned by the loss of the small particle size fraction of the pulps during the chlorite method or the fact that the polysaccharide fractions are damaged, e.g. by oxidative processes, during the respective pulping diminishing the final holocellulose yield. The latter is probably the case in the H_2O_2 pulp, in which the amount of holocellulose is less than half of the total polysaccharide fraction and explains also the lower yield of the H_2O_2 pulp in (Table 9). Such a significant difference can't be explained solely by the additional loss of lignin.

In Figure 10 the main differences when comparing the three kinds of holocellulose can be spotted at wavenumbers ~1730 cm^{-1} and ~1240 cm^{-1}. The first band can be attributed to pectin's and the second to residual lignin (Fasoli et al. 2016).
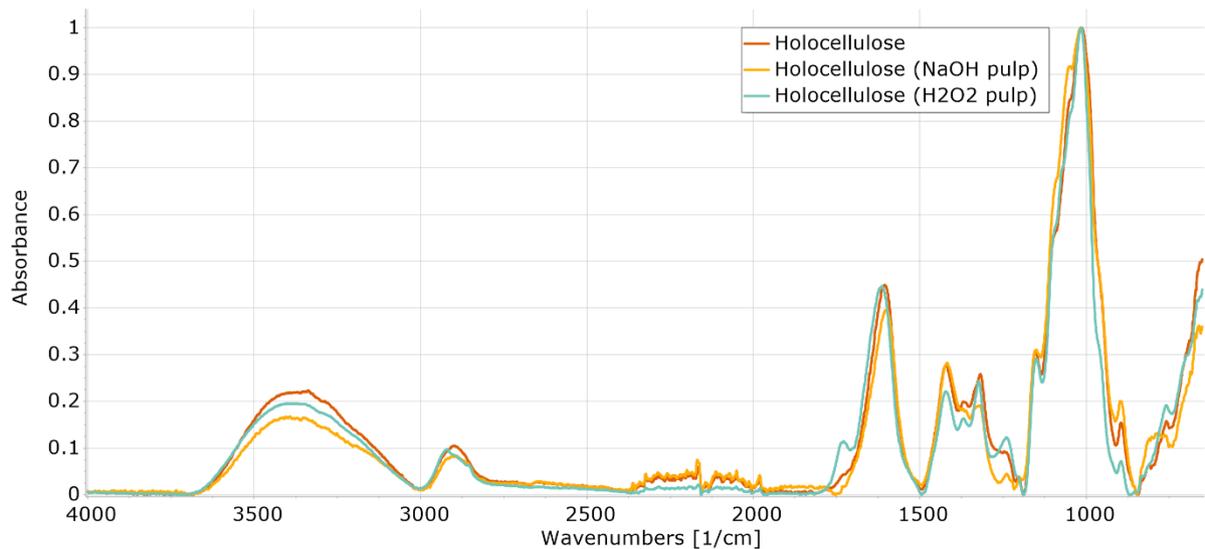
Figure 11: FTIR spectra of holocellulose from native material, NaOH and H$_2$O$_2$ pulp.

In Table 10 a summary of the amounts of the respective components of both pulps is displayed as well as the enrichment or decrease compared to native *M. spicatum* material. For the NaOH pulp the holocellulose content was increased and the monosaccharide composition remained very similar to the original material, with some decrease in galacturonic acid and rhamnose, which equals to a loss of pectin. The H$_2$O$_2$ pulp on the other hand yielded a very different picture: It's low holocellulose content compared to the native *M. spicatum* suggested that the hydrogen peroxide treatment intensely damaged large parts of the cellulose structure through oxidative processes.

*Table 10: Summary of components of NaOH and H$_2$O$_2$ pulp with comparison to the native M. spicatum. *The polysaccharides fraction equals the remaining mass percentage after subtracting the amounts of extractives, lignin, protein and ash.*

Main component	Component	NaOH pulp		H$_2$O$_2$ pulp	
		Amount [%]	Difference to native [%]	Amount [%]	Difference to native [%]
Polysaccharides		63.1		69.1	
	Holocellulose	49.3	+13	32.7	-25
Extractives		7.4	-52	7.2	-53
Lignin		17.3	+59	11.2	+3
	Acid-insoluble lignin	13.3	+120	6.9	+13
	Acid-soluble lignin	4.0	-19	4.3	-12
Protein		4.1	-66	4.3	-64
Ash		8.1	-30	8.2	-31

The large gap between the polysaccharide and holocellulose fraction of the H_2O_2 pulp especially, could be attributed to loss of particles that were weakened by the hydrogen peroxide treatment and consequentially oxidized and washed out in the holocellulose chlorite process. This explanation was further encouraged by the significantly lower yields of the H_2O_2 pulp (34 ± 9) compared to those of the NaOH pulp (50 ± 6 %).

The high increase in acid-insoluble lignin assumed to due to pseudo-lignin, which is formed from carbohydrate and lignin degradation products during pulping.

Steep reductions in protein content as well as extractives were achieved for both pulping processes but could also be further improved upon to potentially additionally increase mechanical stability, storage life and decrease unwanted coloring.

Figure 12 shows paper samples of the NaOH and H_2O_2 pulp. The color of the dry material of the NaOH pulp was dark brown, which is supposedly due to the increase of (pseudo-)lignin. The H_2O_2 pulp, which did not exhibit such a significant increase in acid-insoluble lignin, shifted to a light yellowish green color, apparently giving way to the remainder of the extractives.
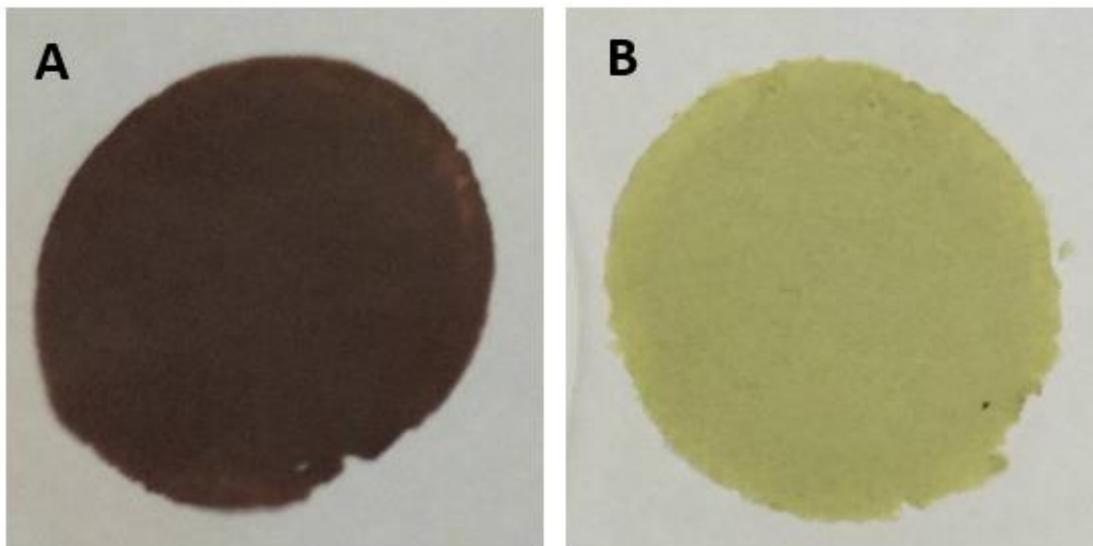

Figure 12: Paper samples made purely from NaOH pulp (A) and from H_2O_2 pulp (B).

3.3   Mechanical analysis

In order to get a reference point for the mechanical properties and stability of the various papers, 5 specimens of the preselected samples were subjected to tensile tests. As a reference for the analysis, a paper sample of unbleached kraft pulp softwood fibers with a Schopper-Riegler value of 43 was used. In addition to the neat samples, blended paper samples were prepared by merging 60 wt% *M. spicatum* pulp with the reference kraft pulp.
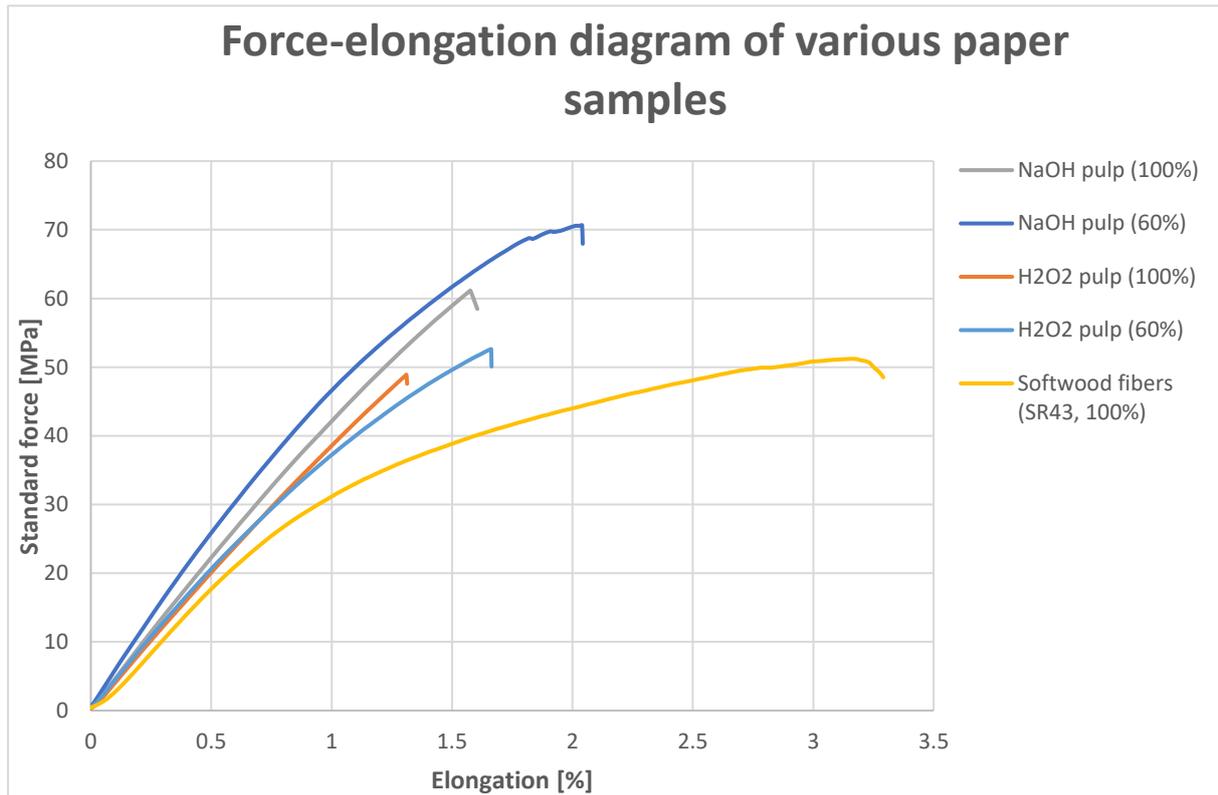

Figure 13: Typical tensile strength measurement results of paper samples made from various pulps and blends.

3.2.1 Comparison of tensile strength measurement results

Figure 13 shows a stress-strain curve with typical tensile strength measurement results of the paper samples with 60 wt% *M. spicatum* pulp. There are two things distinctly noticeable: firstly, the blended paper of 60 % NaOH pulp and 40 % kraft pulp could withstand an impressively high tensile strength (up to 70 N/mm²), even up to 3 % higher when comparing the best results to those of the reference paper. The blended papers at a higher *M. spicatum* pulp ratio (80 %) did not show this effect, yielding results comparable to the pure pulp samples. This suggests a synergistic effect of the two pulps at a certain ratio. Indicating, that *M. spicatum* pulp can increase the available bonding area between the stronger kraft pulp fibers, thus improving the tensile strength.

Secondly, the elongation capabilities of all tested papers were falling behind the pure wood-fiber paper by a significant margin, reaching only up to 60 % to 65 % of the elongation of the reference sample (see Figure 13, Figure 14 A and Figure 15 A). Looking at the point of rupture, all sample papers break cleanly without any yielding of the material, while the reference paper shows a yield point, followed by a short non-linear plastic deformation.
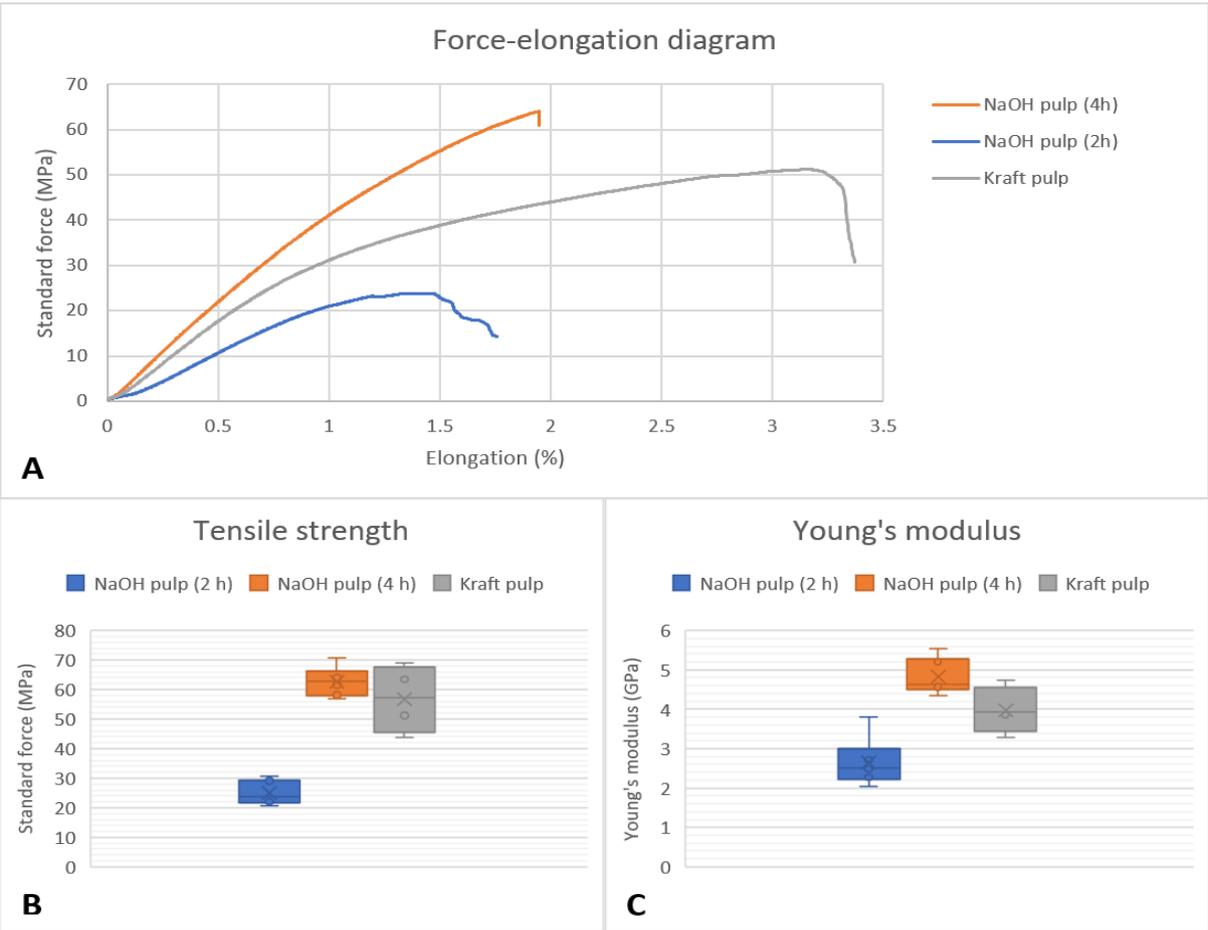

Figure 14: Various diagrams of 60 wt% M. spicatum NaOH pulps after 2 and 4 hours of pulping with kraft pulp as reference; A: Typical force-elongation diagram; B: tensile strength
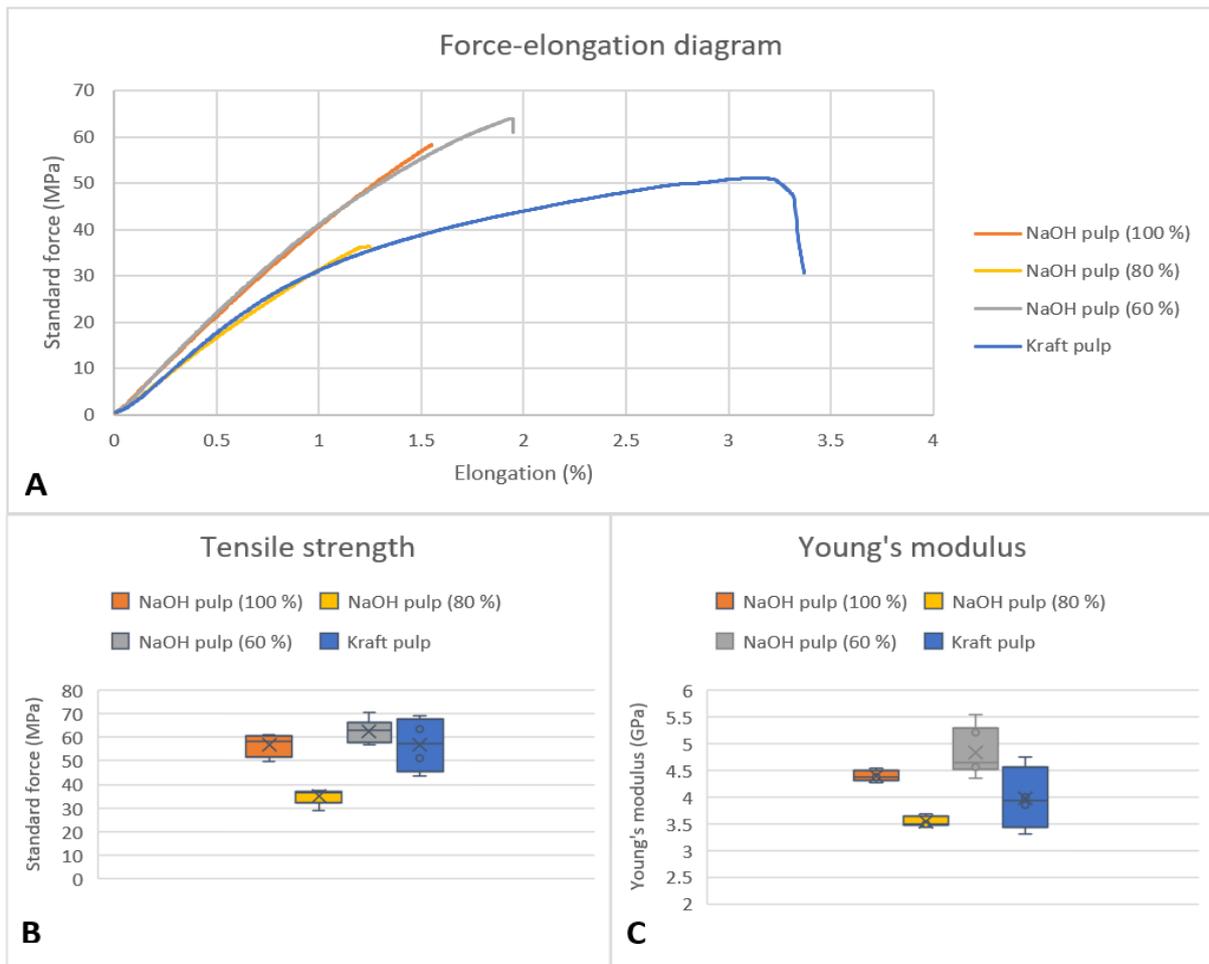
Figure 15: Various diagrams of 60, 80 and 100 wt% M. spicatum NaOH pulps with kraft pulp as reference; A: Typical force-elongation diagram; B: tensile strength box plots; C: young's modulus box plots.

Tensile strength results of NaOH pulp

In Figure 14 the effect of pulping duration on the mechanical properties of the pulp can be observed. The step from 2 h pulping duration to 4 h displayed a drastic improvement of tensile strength as well as Young's modulus.

Papers made from pure NaOH pulp showed high tensile strength results (57 ±4 MPa), reaching results similar to the reference paper (57 ±9 MPa). While the elongation capabilities of the pure NaOH pulp sample reached (1.5 ±1 %) just 42 % of the kraft pulp (3.6 ±3 %). The Young's moduli of the reference and sample were quite similar, 4.0 ±0.5 GPa and 4.4 ±1 GPa respectively, rendering the latter a little stiffer than the former.

Figure 15 B and C show the tensile strength and the Young's modulus results of the blend papers made from 100 %, 80 % and 60 % NaOH pulp and 0 %, 20 % and 40 % soft wood kraft pulp, respectively. The most noticeable outcome here are the results yielded from the blended paper of 60 % NaOH pulp: The tensile strength measurement amounted to 61 ±5 MPa on average, exceeding the reference paper by 4 %, while the Young's modulus amounted to 4.8

±0.4 GPa, thus increasing the stiffness by 21 %. Furthermore, the elongation qualities of the blend improved by 20 % (1.8 ±0.2 %) compared to the pure pulp sample.

Tensile strength results of H_2O_2 pulp

The pure H_2O_2 pulp specimen yielded a tensile strength of 58 ±14 MPa and a Young's modulus of 4.2 ±0.2 GPa, thus achieving very similar results to the reference paper. Elongation-wise, the pure H_2O_2 sample resulted to 1.6 ±0.5 %, which is in the same ballpark as the NaOH pulp. In Figure 16 the blended papers are compared to the pure H_2O_2 pulp variant. Neither regarding tensile strength nor Young's modulus a significant change could be observed, apart from the tensile strength, which did not scatter as much with the addition of kraft pulp.
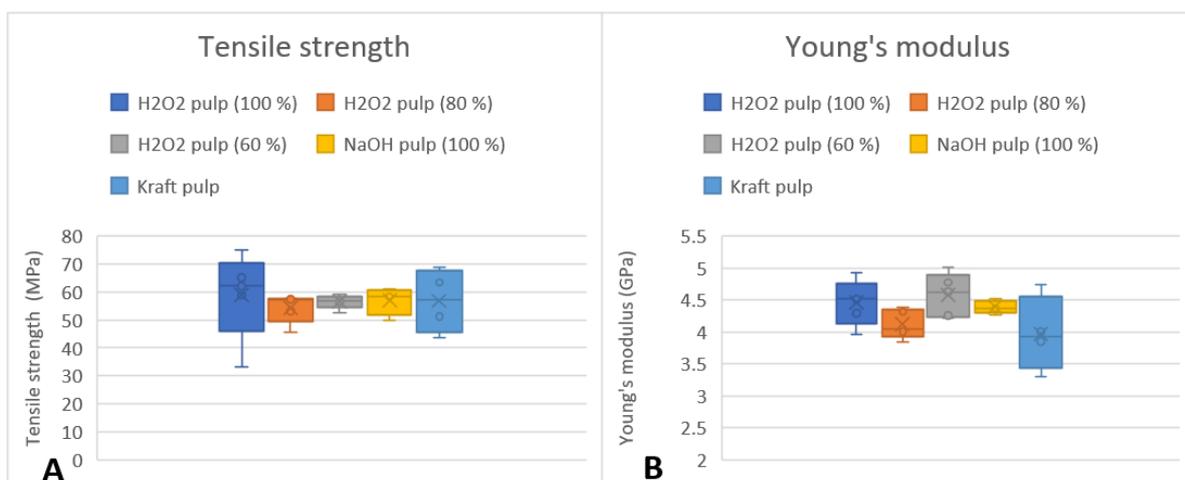

Figure 16: Tensile strength (A) and Young's modulus (B) box plots of 60, 80 and 100 wt% M. spicatum H_2O_2 pulps with NaOH and kraft pulp as reference.

These properties are imparting the papers rather glass-like features (high tensile strength, medium-high stiffness, low elongation capabilities) and will be the main issue to be tackled when thinking about improving the mechanical stability packaging materials.

The pulps and papers of the two most successful treatments (NaOH and H_2O_2 pulping) were then analyzed further. Similar to the native material their macromolecular components were observed to give greater insight as to how the lignocellulosic and pectin composition changes the mechanical properties of the pulps.

Mechanical interaction between fibers and cell clusters

Figure 17 A+B show scanning electron microscope (SEM) images of the blended paper at 500 times magnification. In both pictures fibers and cell clusters are clearly visible.
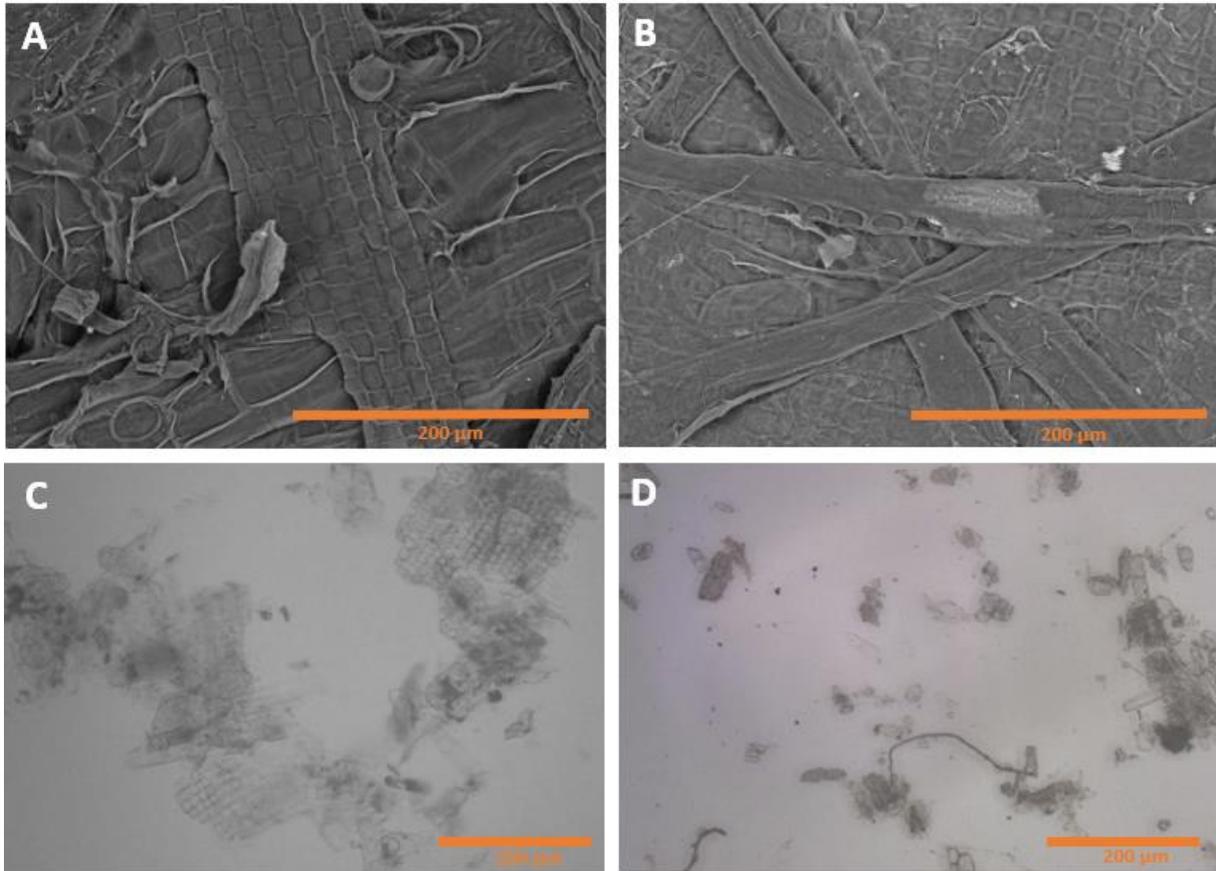

Figure 17: A+B: Blended paper made from 60 % H_2O_2 pulp and 40 % kraft pulp, taken via SEM; papers made from pure NaOH pulp (C) and pure H_2O_2 pulp (D), taken via light microscopy.

The lengthy fibers that are especially visible in Figure 17 C+D originate primarily from the kraft pulp, while the cell clusters can be attributed to the *M. spicatum* pulp.

In addition to the chemical explanation for the improved mechanical properties of the blended material the SEM analysis suggests a kind of hook-and-loop system, where the cell cluster would hook into the wood fibers, thus increasing the tensile strength of the blend.

Chemical additives

Limited tests with chemical additives were conducted in hopes to improve the elongation capabilities especially, as well as to further increase the tensile strength. Cationic starch was introduced as a promising candidate to link to the rather high availability of carboxylic acids, thus crosslinking the fibers, increasing the mechanical properties of the resulting material. In preliminary tests, where the pulps were blended with 5 wt% of cationic starch, elongation capabilities could not be improved, but a slight enhancement of tensile strength for both pulps could be achieved (+10-15 %). Other additives like the addition of 5 wt% of chitosan, did not yield any noticeable improvements to the material's mechanical properties.

3.4   Methane potential and degradation kinetics

To further investigate the added value potential of *M. spicatum* biomass biogas experiments were carried out, results of which are shown below:
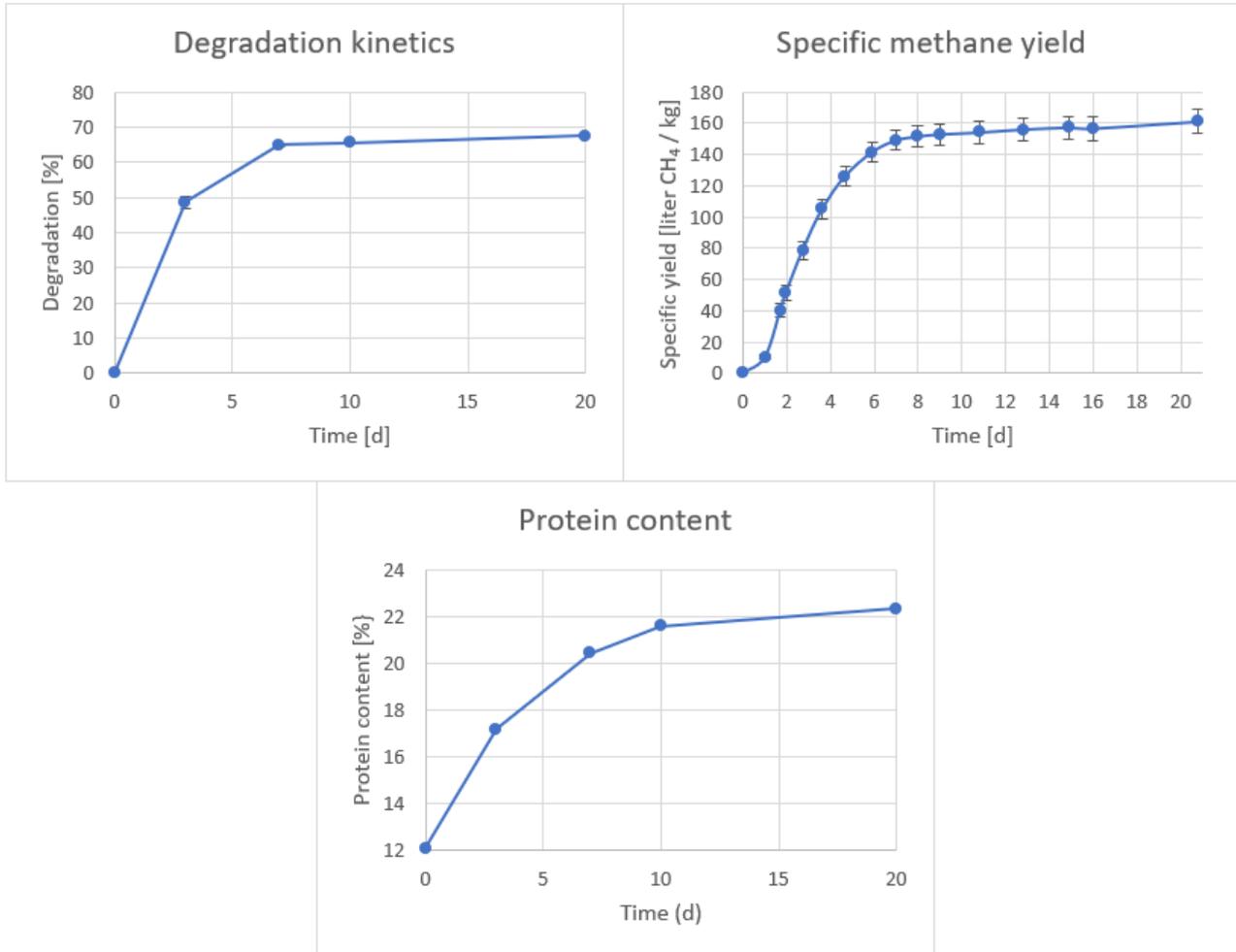

Figure 18: Several diagrams of the biogas experiment of M. spicatum over a period of 20 days: degradation kinetics (A), specific methane yield (B), protein content (C).

The methane potential experiment (Figure 18 B) yielded a maximum specific biogas yield of 321 l_N kg^{-1} ODM ± 15 l_N kg^{-1} ODM and a maximum specific methane yield of 161 l_N kg^{-1} ODM ± 8 l_N kg^{-1} ODM. These results are rather moderate rendering substrate of *M. spicatum* close to the methane yields of yard waste (183 l_N kg^{-1} ODM (Li et al. 2013)). For comparison, the methane potential of wheat straw could result to 245 l_N kg^{-1} ODM (Li et al. 2013).

The degradation kinetics (Figure 18 A) showed that a maximum of 67 ±<1 % would be metabolized by the microorganisms, the rest could be assumed to be inorganics, lignin and inaccessible lignocellulosic complexes.

Furthermore, the protein content of each degradation stage (Figure 18 C) was analyzed via elementary analysis. It showed a similar trend to the degradation kinetics and the methane

yield and was assumed to be due to the preferential microbial metabolization of polysaccharides. To a lesser degree, the growth of the microorganisms and their protein synthesis could have contributed to the steadily increasing protein content, though a wash-out thereof could be assumed.

Tensile strength testing of each stage yielded increasingly weak papers which matches the findings above, due to a decrease in cellulose and an inversely proportional increase in protein. These moderate methane yields and high amounts of non-fermentable residues align with the thesis of Li et al. 2013, that higher lignin contents could lead to an impaired methane yield.

Both the methane potential graph (Figure 18 B) as well as the degradation kinetics graph (Figure 18 A) very much represent typical bacterial batch growth phases, with day 0-1 as lag phase, where bacteria adapt to their environment with the production of necessary cell components, thus little growth and production of metabolites (part of which is the target compound methane) occurs. From day 1-4 the log phase was undergone with high bacterial growth and metabolite production due to plentiful substrate availability. Starting from day 7 a decline of growth could be observed which signalized a beginning shortage of readily available substrate and an accumulation of metabolites. This led into the stationary phase from day 7 where the growth rate and death rate were counterbalancing each other, and production of methane decreased.

These graphs reflect the combined characteristics, e.g. specific growth rate, of manifold bacterial species that were present in the inoculum dealing with *M. spicatum* as substrate (Fuchs, Schlegel, and Eitinger 2007).

4.   Conclusion

In this researched we have unraveled the macromolecular components of *Myriophyllum spicatum*: besides a rather high holocellulose content, which is important for potential wood replacement efforts, a relatively high amount of pectin could be confirmed. Pectin has interesting chemical properties including carboxyl functional groups which could be investigated in the future.

Furthermore lignin, which is absent in many comparable water plants and only present in a few algae was shown to be present (Martone et al. 2009).

With the macromolecular constituents of *Myriophyllum spicatum* quantified, many pulping possibilities have been explored and two candidates have been selected for further investigation.

Both pulping processes were conducted in mild conditions using cheap, non-toxic und ubiquitous chemicals, and could therefore present a straight-forward and environmentally friendly replacement to conventional wood pulps.

The NaOH pulp variant revealed high tensile strength properties, very much comparable to the pure softwood kraft pulp reference. In a blend with the reference pulp, it showed increased mechanical properties to the pure pulps; suggesting a synergetic effect.

The H_2O_2 pulp variant achieved similarly high tensile strength results but was obtained at a significant lower yield of 34 %, which is 32 % lower in comparison to the NaOH pulp yield. While the pulping experiments were very promising, additional research and optimization is necessary to make *M. spicatum* a marketable alternative to wood in the time to come.

The future issues that will have to be tackled concerning pulping are, the low pulping yields and the rather high lignin content (a result of pseudo-lignin formation during pulping) which could prove problematic, especially when color and brightness are of importance. Our results suggest that the complex composition of the plant has to be considered to tackle these issues and to avoid side-reactions during pulping, which can be induced e.g. by the high amount of protein and extractives. Secondly, the brittleness of the materials and their comparably low elongation at break values has to be overcome for packaging applications. This issue could possibly be solved by including additives to the process to improve the mechanical properties of the pulp.

In addition, the potential for energy utilization was evaluated by using the plant as a substrate for biogas conversion. The methane volume gained per organic dry matter was moderate, but it could be a potentially more beneficial alternative to the city of Vienna than the current sole utilization of the plant in composting.

Taking this into account, *Myriophyllum spicatum* offers excellent possibilities for added value products combined with its world-wide abundance and fast growth it is a very promising candidate for environmentally friendly, inexpensive and easily accessible source material for modern biorefinery approaches.

References:

Buchanan, Bob B., Wilhelm Gruissem, and Russel L. Jones. 2015. *Biochemistry & Molecular Biology of Plants*.

"COMMISSION REGULATION (EC) No 1881/2006 of 19 December 2006 Setting Maximum Levels for Certain Contaminants in Foodstuffs." n.d.

"Council of Europe - Resolution Ap (2002) on Paper and Board Materials and Articles Intended to Come into Contact with Food Stuffs." n.d.

Dinwoodie, J.M. 1989. *Wood, Nature's Cellular, Polymeric, Fibre-Composite*.

Fasoli, Marianna, Rossana Dell'Anna, Silvia Dal Santo, Raffaella Balestrini, Andrea Sanson, Mario Pezzotti, Francesca Monti, and Sara Zenoni. 2016. "Pectins, Hemicelluloses and Celluloses Show Specific Dynamics in the Internal and External Surfaces of Grape Berry Skin During Ripening." *Plant and Cell Physiology* 57 (6): 1332–49. https://doi.org/10.1093/pcp/pcw080.

Florence, T M. 1980. "Degradation of Protein Disulphide Bonds in Dilute Alkali." *Biochemical Journal* 189 (3): 507–20. https://doi.org/10.1042/bj1890507.

Fuchs, Georg, Hans Günter Schlegel, and Thomas Eitinger, eds. 2007. *Allgemeine Mikrobiologie: 53 Tabellen*. 8., vollst. überarb. und erw. Aufl. Stuttgart: Thieme.

Harris, J.F., A.J. Baker, and A.H Conner. 1985. *Two-Stage Dilute Sulfuric Acid Hydrolysis of Wood: An Investigation of Fundamentals*.

Harrysson, Hanna, Maria Hayes, Friederike Eimer, Nils-Gunnar Carlsson, Gunilla B. Toth, and Ingrid Undeland. 2018. "Production of Protein Extracts from Swedish Red, Green, and Brown Seaweeds, Porphyra Umbilicalis Kützing, Ulva Lactuca Linnaeus, and Saccharina Latissima (Linnaeus) J. V. Lamouroux Using Three Different Methods." *Journal of Applied Phycology*, April. https://doi.org/10.1007/s10811-018-1481-7.

He, Yan, Qiao-Hong Zhou, Bi-Yun Liu, Long Cheng, Yun Tian, Yong-Yuan Zhang, and Zhen-Bin Wu. 2016. "Programmed Cell Death in the Cyanobacterium Microcystis Aeruginosa Induced by Allelopathic Effect of Submerged Macrophyte Myriophyllum Spicatum in Co-Culture System." *Journal of Applied Phycology* 28 (5): 2805–14. https://doi.org/10.1007/s10811-016-0814-7.

Kantouch, A., A. Hebeish, and M.H. El-Rafie. 1970. "Action of Sodium Chlorite on Cellulose and Cellulose Derivatives." *Textile Research Journal* 40 (2): 178–84. https://doi.org/10.1177/004051757004000211.

Keskinkan, O., M.Z.L. Goksu, M. Basibuyuk, and C.F. Forster. 2004. "Heavy Metal Adsorption Properties of a Submerged Aquatic Plant (Ceratophyllum Demersum)." *Bioresource Technology* 92 (2): 197–200. https://doi.org/10.1016/j.biotech.2003.07.011.

Li, Yeqing, Ruihong Zhang, Guangqing Liu, Chang Chen, Yanfeng He, and Xiaoying Liu. 2013. "Comparison of Methane Production Potential, Biodegradability, and Kinetics of Different Organic Substrates." *Bioresource Technology* 149 (December): 565–69. https://doi.org/10.1016/j.biortech.2013.09.063.

Lin, S.Y. 1992. "Methods in Lignin Chemistry. Springer Series in Wood Science." Springer.

Marko, Michelle D., Elisabeth M. Gross, Raymond M. Newman, and Florence K. Gleason. 2008. "Chemical Profile of the North American Native Myriophyllum Sibiricum Compared to the Invasive M. Spicatum." *Aquatic Botany* 88 (1): 57–65. https://doi.org/10.1016/j.aquabot.2007.08.007.

Martone, Patrick T., José M. Estevez, Fachuang Lu, Katia Ruel, Mark W. Denny, Chris Somerville, and John Ralph. 2009. "Discovery of Lignin in Seaweed Reveals Convergent Evolution of Cell-Wall Architecture." *Current Biology* 19 (2): 169–75. https://doi.org/10.1016/j.cub.2008.12.031.

Moody, Michael L., Nayell Palomino, Philip S.R. Weyl, Julie A. Coetzee, Raymond M. Newman, Nathan E. Harms, Xing Liu, and Ryan A. Thum. 2016. "Unraveling the Biogeographic Origins of the Eurasian Watermilfoil (*Myriophyllum Spicatum*) Invasion in North America." *American Journal of Botany* 103 (4): 709–18. https://doi.org/10.3732/ajb.1500476.

Mortha, Gérard, Jennifer Marcon, David Dallérac, Nathalie Marlin, Christophe Vallée, Nadège Charon, and Agnès Le Masle. 2015. "Depolymerization of Cellulose during Cold Acidic Chlorite Treatment." *Holzforschung* 69 (6): 731–36. https://doi.org/10.1515/hf-2014-0270.

Murphy, Kevin. 2018. "Invasive Species Compendium: Myriophyllum Spicatum (Spiked Watermilfoil)." Centre for Agriculture and Bioscience International.

Mussatto, Solange I., George J. M. Rocha, and Inês C. Roberto. 2008. "Hydrogen Peroxide Bleaching of Cellulose Pulps Obtained from Brewer's Spent Grain." *Cellulose* 15 (4): 641–49. https://doi.org/10.1007/s10570-008-9198-4.

Nakai, S. 2000. "Myriophyllum Spicatum-Released Allelopathic Polyphenols Inhibiting Growth of Blue-Green Algae Microcystis Aeruginosa." *Water Research* 34 (11): 3026–32. https://doi.org/10.1016/S0043-1354(00)00039-7.

Ragnar, Martin, Gunnar Henriksson, Mikael E. Lindström, Martin Wimby, Jürgen Blechschmidt, and Sabine Heinemann. 2014. "Pulp." In *Ullmann's Encyclopedia of Industrial Chemistry*, edited by Wiley-VCH Verlag GmbH & Co. KGaA, 1–92. Weinheim, Germany: Wiley-VCH Verlag GmbH & Co. KGaA. https://doi.org/10.1002/14356007.a18_545.pub4.

Rıdvan Sivaci, E, Aysel Sivaci, and Münevver Sökmen. 2004. "Biosorption of Cadmium by Myriophyllum Spicatum L. and Myriophyllum Triphyllum Orchard." *Chemosphere* 56 (11): 1043–48. https://doi.org/10.1016/j.chemosphere.2004.05.032.

Rogoff, Marc J., and Francois Screve. 2019. "Energy From Waste Technology." In *Waste-To-Energy*, 29–56. Elsevier. https://doi.org/10.1016/B978-0-12-816079-4.00003-7.

Rowell, Roger M. 2013. *Handbook of Wood Chemistry and Wood Composites*. 2nd ed.

Shao, Zhuoping, and Fuli Wang. 2018. "Mechanical Characteristics and Stress–Strain Relationship of Wood Structure." In *The Fracture Mechanics of Plant Materials*, by Zhuoping Shao and Fuli Wang, 11–26. Singapore: Springer Singapore. https://doi.org/10.1007/978-981-10-9017-2_2.

Shinde, Somnath D., Xianzhi Meng, Rajeev Kumar, and Arthur J. Ragauskas. 2018. "Recent Advances in Understanding the Pseudo-Lignin Formation in a Lignocellulosic Biorefinery." *Green Chemistry* 20 (10): 2192–2205. https://doi.org/10.1039/C8GC00353J.

Smith, Robert M., and David E. Hansen. 1998. "The PH-Rate Profile for the Hydrolysis of a Peptide Bond." *Journal of the American Chemical Society* 120 (35): 8910–13. https://doi.org/10.1021/ja9804565.

Södergård, Anders, and Mikael Stolt. 2010. "Industrial Production of High Molecular Weight Poly(Lactic Acid)." In *Poly(Lactic Acid)*, edited by Rafael Auras, Loong-Tak Lim, Susan E. M. Selke, and Hideto Tsuji, 27–41. Hoboken, NJ, USA: John Wiley & Sons, Inc. https://doi.org/10.1002/9780470649848.ch3.

Stanley, Ronald A. 1974. "Toxicity of Heavy Metals and Salts to Eurasian Watermilfoil (Myriophyllum Spicatum L.)." *Archives of Environmental Contamination and Toxicology* 2 (4): 331–41. https://doi.org/10.1007/BF02047098.

Sundheq, Anna, Kenneth Sundherg, Camilla Lillandt, and Bjarne Holmhom. 1996. "Determination of Hemicelluloses and Pectins in Wood and Pulp Fibres by Acid Methanolysis and Gas Chromatography." *Nordic Pulp & Paper Research Journal* 11 (4): 216–19. https://doi.org/10.3183/npprj-1996-11-04-p216-219.

"TAPPI Test Method T 12 Wd-82, Preparation of Wood for Chemical Analysis (Including Procedures for Removal of Extractive and Determination of Moisture Content)." n.d.

"TAPPI Test Method *T 211 Om-12, Ash in Wood, Pulp, Paper, and Paperboard: Combustion at 525°C." n.d.

"TAPPI Test Method T222 Om-88, Acid-Insoluble Lignin in Wood and Pulp." n.d.

Van Alfen, Neal K. 2014. "Encyclopedia of Agriculture and Food Systems, Second Edition.Pdf."

Wiener Gewässer (Magistratsabteilung 45). 2019. "Mähen von Unterwasserpflanzen in Der Alten Donau," 2019.

Zhao, Jian, Xuezhi Li, Yinbo Qu, and Peiji Gao. 2004. "Alkaline Peroxide Mechanical Pulping of Wheat Straw With Enzyme Treatment." *Applied Biochemistry and Biotechnology* 112 (1): 13–24. https://doi.org/10.1385/ABAB:112:1:13.